Inorg. Chem. **2007**, *46*, 465–485

Functionalized Bis(thiosemicarbazonato) Complexes of Zinc and Copper: Synthetic Platforms Toward Site-Specific Radiopharmaceuticals

Jason P. Holland,[†] Franklin I. Aigbirhio,[‡] Helen M. Betts,[†] Paul D. Bonnitcha,[†] Paul Burke,[‡] Martin Christlieb,[†] Grant C. Churchill,[§] Andrew R. Cowley,[†] Jonathan R. Dilworth,*[,†] Paul S. Donnelly,[||] Jennifer C. Green,[†] Josephine M. Peach,[†] Sridhar R. Vasudevan,[§] and John E. Warren[⊥]

Chemistry Research Laboratory, Department of Chemistry, University of Oxford, 12 Mansfield Road, Oxford OX1 3TA, United Kingdom, Wolfson Brain Imaging Centre, Department of Clinical Neurosciences, University of Cambridge, Addenbrooke's Hospital, Cambridge CB2 2QQ, United Kingdom, Department of Pharmacology, University of Oxford, Mansfield Road, Oxford OX1 3QT, United Kingdom, School of Chemistry, University of Melbourne, Parkville, Victoria 3010, Australia, and CCLRC Daresbury Laboratory, Daresbury, Warrington WA4 4AD, United Kingdom

Received August 17, 2006

Two new types of unsymmetrical bis(thiosemicarbazone) proligands and their neutral zinc(II) and copper(II) complexes have been synthesized. These bifunctional ligands both chelate the metal ions and provide pendent amino groups that can be readily functionalized with biologically active molecules. Functionalization has been demonstrated by the synthesis of three water-soluble glucose conjugates of the new zinc(II) bis(thiosemicarbazonato) complexes, and their copper(II) analogues have been prepared in aqueous solution via transmetalation. A range of techniques including NMR, electron paramagnetic resonance, cyclic voltammetry, high-performance liquid chromatography (HPLC), UV/vis, and fluorescence emission spectroscopy have been used to characterize the complexes. Four compounds, including two zinc(II) complexes, have been characterized by X-ray crystallography. The connectivity and conformation of the glucose conjugates have been assigned by NMR spectroscopy. Time-dependent density functional theory calculations have been used to assign the electronic transitions of the copper(II) bis(thiosemicarbazonato) chromophore. Two copper-64-radiolabeled complexes, including one glucose conjugate, have been prepared and characterized using radio-HPLC, and transmetalation is shown to be a viable method for radiolabeling compounds with copper radionuclides. Preliminary cell washout studies have been performed under normoxic conditions, and the uptake and intracellular distribution have been studied using confocal fluorescence microscopy.

Introduction

Over recent years, advances in imaging technology and the potential of nuclear medicine to provide site-specific therapy have generated intense interest in the design of new imaging agents.[1−4] Since Brownell and Sweet[5,6] recorded the first medical images of localized brain tumors using positrons in 1953 and the development of the metabolic imaging agent [^{18}F]-2-fluoro-2-deoxy-D-glucose (^{18}FDG), during the 1970s, the use of positron emission tomography (PET) as a diagnostic tool has expanded rapidly.[7−10] Although other imaging techniques such as computerized tomography (CT)

* To whom correspondence should be addressed. E-mail: jon.dilworth@chem.ox.ac.uk. Tel: +44 (0)1865 285151.
[†] Department of Chemistry, University of Oxford.
[‡] University of Cambridge.
[§] Department of Pharmacology, University of Oxford.
[||] University of Melbourne.
[⊥] CCLRC Daresbury Laboratory.

(1) Smith, S. V. *J. Inorg. Biochem.* **2004**, *98* (11), 1874.
(2) Blower, P. J.; Lewis, J. S.; Zweit, J. *Nucl. Med. Biol.* **1996**, *23* (8), 957.
(3) Anderson, C. J.; Welch, M. J. *Chem. Rev.* **1999**, *99* (9), 2219.
(4) Volkert, W. A.; Hoffman, T. J. *Chem. Rev.* **1999**, *99* (9), 2269.
(5) Brownell, G. L.; Sweet, W. H. *Nucleonics* **1953**, *11*, 40.
(6) Sweet, W. H. *N. Eng. J. Med.* **1951**, *245*, 875.
(7) Wrenn, F. R., Jr.; Good, M. L.; Handler, P. *Science* **1951**, *113* (2940), 525.
(8) Adam, M. J.; Wilbur, D. S. *Chem. Soc. Rev.* **2005**, *34* (2), 153.
(9) Gallagher, B. M.; Ansari, A.; Atkins, H.; Casella, V.; Christman, D. R.; Fowler, J. S.; Ido, T.; MacGregor, R. R.; Som, P.; Wan, C. N.; Wolf, A. P.; Kuhl, D. E.; Reivich, M. *J. Nucl. Med.* **1977**, *18* (10), 990.
(10) Gallagher, B. M.; Fowler, J. S.; Gutterson, N. I.; MacGregor, R. R.; Wan, C. N.; Wolf, A. P. *J. Nucl. Med.* **1978**, *19* (10), 1154.

10.1021/ic0615628 CCC: $37.00
Published on Web 12/22/2006

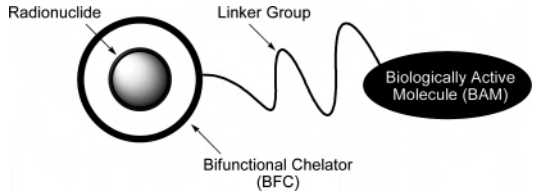

Figure 1. Schematic representation of the conjugation of an encapsulated radionuclide to a BAM via a linker group.

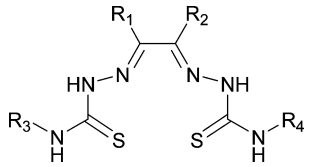

Figure 2. General structure of the bis(thiosemicarbazone) proligands. Neutral complexes with zinc(II) and copper(II) ions are formed after double deprotonation to give the bis(thiosemicarbazonato) ligand.

and magnetic resonance imaging (MRI) have superior spatial resolution ($\leq$1 mm vs 3−10 mm for PET), they suffer from much lower sensitivity, usually requiring the use of contrast agents at concentrations that may be toxic to the patient.[1] In comparison, the increased sensitivity derived from the coincident detection of two annihilation γ-ray photons (511 keV) means only nanomolar concentrations of a radiopharmaceutical need be administered to obtain an image using PET.[11] However, the principle advantage of PET imaging is the ability to provide the clinician with more than the structural information from CT and MRI by correlation of the observed biodistribution of an imaging agent with cellular biochemistry. The mechanisms by which an administered drug may tend to localize in different tissue phenotypes is dependent on the molecular properties of the radiopharmaceutical, for example, lipophilicity, molecular weight, planarity, pK_a, and redox potentials.[12,13] Such structure−activity relationships provide the opportunity for the rational design of ever more site-specific radiopharmaceuticals.

An important concept often cited in the context of radiopharmaceutical chemistry is that of bioconjugation, as illustrated in Figure 1.[1,2,14] Bioconjugation involves the coupling of a radionuclide to a biologically active molecule (BAM) through the use of a bifunctional chelator (BFC) with a linker atom or group. This methodology has many subtleties associated with both the synthesis and design of such complex bioinorganic systems. Aspects include the choice of the radionuclide, the construction of the ligand, metal complexation, the nature of the linker group, and the reaction sequence and type of coupling chemistry used to combine the radionuclide with the chosen BAM.[1] The precise design of the system will primarily be governed by the intended target and desired application. A common assumption used in the bioconjugation methodology is the idea that the targeting and imaging or therapeutic properties of a compound can be and assigned to different parts of the molecule: the BAM and radionuclide groups, respectively. Even though this assumption is not strictly valid (such as, for example, the modification of a protein via coupling may lead to structural distortion and a loss of affinity for a receptor site), it does facilitate synthesis and offers the potential to develop a radiopharmaceutical "tool kit". The development of a library of radionuclides, BFCs, and targeting groups combined with versatile synthetic protocols for coupling of the encapsulated radionuclides to different BAMs represents a major goal of radiopharmaceutical design.[2]

Despite the attraction of delivering a radionuclide to a target using biomolecules to confer site-directing properties, difficulties often arise in developing a reliable coupling scheme to connect the BFC with different bioactive molecules. However, in several elegant procedures, Schibli et al. demonstrated that glucose and 2-deoxyglucose may be modified at the C-1, C-2, C-3, and C-6 positions using standard organic chemistry to construct an ethylene-spaced tridentate ligand set.[15−18] Subsequent complexation to technetium(I) and rhenium(I) using $[M(CO)_3(H_2O)_3]^+$, where M = Re or Tc, proceeded rapidly in >90% yield, giving kinetically stable, low-spin d^6 complexes. However, initial in vivo experiments revealed a low accumulation of the C-1-functionalized complexes in cancerous cells. This is most likely due to the fact that the anomeric C-1 hydroxyl group is important for recognition of glucose by Glut1, the main glucose transporter protein in humans. There is evidence that modification of glucose at the C-3 and C-6 positions is tolerated.[17] Recently, Storr et al. have designed alternative carbohydrate-based systems incorporating the $[M(CO)_3]^+$ core.[19−22]

Copper complexes of bis(thiosemicarbazonato) ligands (Figure 2) represent a class of compounds that have recently been the subject of intense research because of their potential as radiopharmaceuticals for the specific targeting of hypoxic tissue.[23−29] Hypoxia is a pathological condition that has been associated with stroke, heart disease, and certain types of cancer. The ability to image and measure the extent of hypoxia noninvasively in vivo would greatly assist the clinical management of these and other diseases.[13] Bis(thiosemicarbazonato) complexes with long-chain fatty acid substituents on the backbone (R_1 and R_2) have been made.[2] However, no general methods for the conjugation of BAMs

(11) Laforest, R.; Dehdashti, F.; Lewis, J. S.; Schwarz, S. W. *Eur. J. Nucl. Med. Mol. Imaging* **2005**, *32* (7), 764.
(12) Dearling, J. L. J.; Blower, P. J. *Chem. Commun.* **1998**, 2531.
(13) Dearling, J. L. J.; Lewis, J. S.; Mullen, G. E. D.; Welch, M. J.; Blower, P. J. *J. Biol. Inorg. Chem.* **2002**, *7* (3), 249.
(14) Rogers, B. E.; Anderson, C. J.; Connett, J. M.; Guo, L. W.; Edwards, W. B.; Sherman, E. L. C.; Zinn, K. R.; Welch, M. J. *Bioconjugate Chem.* **1996**, *7* (4), 511.
(15) Petrig, J.; Schibli, R.; Dumas, C.; Alberto, R.; Schubiger, P. A. *Chem.—Eur. J.* **2001**, *7* (9), 1868.
(16) Dumas, C.; Schibli, R.; Schubiger, P. A. *J. Org. Chem.* **2003**, *68* (2), 512.
(17) Dumas, C.; Petrig, J.; Frei, L.; Spingler, B.; Schibli, R. *Bioconjugate Chem.* **2005**, *16* (2), 421.
(18) Schibli, R.; Dumas, C.; Petrig, J.; Spadola, L.; Scapozza, L.; Garcia-Garayoa, E.; Schubiger, P. A. *Bioconjugate Chem.* **2005**, *16* (1), 105.
(19) Storr, T.; Fisher, C. L.; Mikata, Y.; Yano, S.; Adam, M. J.; Orvig, C. *Dalton Trans.* **2005**, 654.
(20) Storr, T.; Obata, M.; Fisher, C. L.; Bayly, S. R.; Green, D. E.; Brudzinska, I.; Mikata, Y.; Patrick, B. O.; Adam, M. J.; Yano, S.; Orvig, C. *Chem.—Eur. J.* **2005**, *11* (1), 195.
(21) Storr, T.; Sugai, Y.; Barta, C. A.; Mikata, Y.; Adam, M. J.; Yano, S.; Orvig, C. *Inorg. Chem.* **2005**, *44* (8), 2698.
(22) Bayly, S. R.; Fisher, C. L.; Storr, T.; Adam, M. J.; Orvig, C. *Bioconjugate Chem.* **2004**, *15* (4), 923.

Scheme 1. General Reaction Scheme for the Synthesis of Unsymmetrical Zinc(II) Bis(thiosemicarbazonato) Complexes **12**−**17**[a]

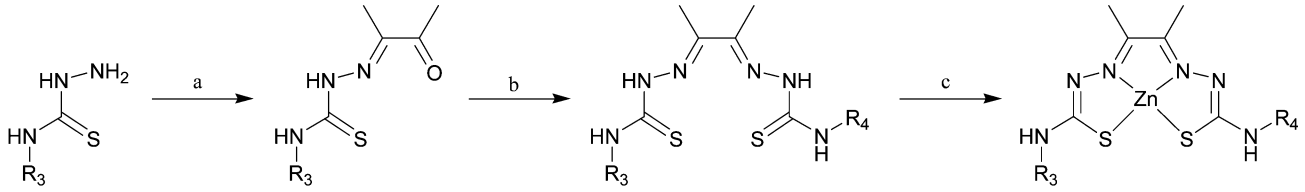

1 R_3 = allyl

2 R_3 = Me, 89%
3 R_3 = Et, 84%
4 R_3 = Ph, 88%
5 R_3 = allyl, 76%

6 R_3 = Me, $R_4 = NH_2$, 93%
7 R_3 = Et, $R_4 = NH_2$, 89%
8 R_3 = Ph, $R_4 = NH_2$, 78%
9 R_3 = allyl, $R_4 = NH_2$, 84%
10 R_3 = allyl, R_4 = Me, 89%
11 R_3 = allyl, R_4 = Et, 95%

12 R_3 = Me, $R_4 = NH_2$, 97%
13 R_3 = Et, $R_4 = NH_2$, 95%
14 R_3 = Ph, $R_4 = NH_2$, 89%
15 R_3 = allyl, $R_4 = NH_2$, 83%
16 R_3 = allyl, R_4 = Me, 93%
17 R_3 = allyl, R_4 = Et, 96%

[a] (a) 2,3-Butadione, concentrated HCl catalyst, water, <1 h. (b) Thiocarbohydrazide or 4-*N*-alkyl-3-thiosemicarbazide, 10% HCl(aq) catalyst, ethanol, reflux, 5 h. (c) $Zn(OAc)_2 \cdot 2H_2O$, methanol, reflux, 4 h.

to bis(thiosemicarbazonato) complexes have been reported. Therefore, there is a need to develop new complexes that can be readily functionalized with a diverse range of biomolecules.

The zinc(II) complexes of bis(thiosemicarbazonato) ligands are important for two main reasons. First, the complexes are diamagnetic. This facilitates the characterization of new ligand systems and complexes through the use of NMR. Second, the zinc(II) complexes were found to be weakly fluorescent.[30] Fluorescence microscopy has already been used to track the uptake and intracellular distribution of several zinc(II) bis(thiosemicarbazonato) complexes in different cancer cell lines.[31] Knowledge of the intracellular distribution of these complexes is crucial in the design of compounds that not only are selective for particular tissue phenotypes but also target specific organelles.[11]

This paper describes the synthesis and full characterization of a series of new unsymmetrical bis(thiosemicarbazone) proligands derived from 2,3-butadione. For each new ligand, the synthesis proceeds via isolation of the corresponding monoketothiosemicarbazone species, which facilitates the construction of unsymmetrical systems. The zinc(II) complexes of all ligands and several copper(II) complexes are described. Four crystal structures, including two zinc(II) complexes, have been obtained. The principle of bioconjugation is demonstrated by the synthesis of three glucose-functionalized complexes. Where possible, full spectroscopic and electrochemical data have been acquired and the kinetics of transmetalation have been studied using stopped-flow experiments. The energetics of zinc(II)/copper(II) exchange have been calculated using density functional theory (DFT). Time-dependent DFT (TD-DFT) calculations have been used to probe the nature of the electronic transitions, and the results are compared with experiments. Preliminary copper-64 radiolabeling experiments have been performed including cell uptake and washout studies under normoxic conditions. Cellular uptake in human IGROV ovarian cancer cells is assessed using confocal fluorescence microscopy.

Results and Discussion

Nomenclature. The following nomenclature is proposed as a simple extension of that already used in the literature. Here the acronym H_2ATSR_3/R_4 is used to indicate an unsymmetrical proligand derived from 2,3-butadione, where $R_1 = R_2$ = methyl (Figure 2). The neutral metal(II) complex of a generic unsymmetrical bis(thiosemicarbazonato) ligand is denoted by $MATSR_3/R_4$, where the ligand is doubly deprotonated and the prefix M = Zn or Cu. For example, H_2ATSM/A and ZnATSE/A refer to compounds **6** and **13**, and the suffixes M/A and E/A are equivalent to methyl/amino and ethyl/amino, respectively (Scheme 1). The proligand precursors, compounds **2**−**5**, are colloquially referred to as monoketothiosemicarbazones.

Synthesis. Since the 1950s, a diverse range of bis(thiosemicarbazonato) ligands and their corresponding metal complexes have been synthesized.[32,33] Symmetric complexes are relatively simple to make. However, the synthesis of unsymmetrical ligands (where $R_1 \neq R_2$ and/or $R_3 \neq R_4$) has proved difficult to control, frequently yielding statistical mixtures and cyclic byproducts.[34−38] The extremely low solubility of the proligands in most common solvents makes

(23) Fujibayashi, Y.; Taniuchi, H.; Yonekura, Y.; Ohtani, H.; Konishi, J.; Yokoyama, A. *J. Nucl. Med.* **1997**, *38* (7), 1155.
(24) Lewis, J. S.; McCarthy, D. W.; McCarthy, T. J.; Fujibayashi, Y.; Welch, M. J. *J. Nucl. Med.* **1999**, *40* (1), 177.
(25) Lewis, J. S.; Sharp, T. L.; Laforest, R.; Fujibayashi, Y.; Welch, M. J. *J. Nucl. Med.* **2001**, *42* (4), 655.
(26) Lewis, J. S.; Welch, M. J. In *Technetium, Rhenium and Other Metals in Chemistry and Nuclear Medicine 6*; Nicolini, M., Mazzi, U., Eds.; Servizi Grafici Editoriali: Padova, Italy, 2002; pp 23−33.
(27) Burgman, P.; O'Donoghue, J. A.; Lewis, J. S.; Welch, M. J.; Humm, J. L.; Ling, C. C. *Nucl. Med. Biol.* **2005**, *32* (6), 623.
(28) O'Donoghue, J. A.; Zanzonico, P.; Pugachev, A.; Wen, B.; Smith-Jones, P.; Cai, S.; Burnazi, E.; Finn, R. D.; Burgman, P.; Ruan, S.; Lewis, J. S.; Welch, M. J.; Ling, C. C.; Humm, J. L. *Int. J. Radiat. Oncol. Biol. Phys.* **2005**, *61* (5), 1493.
(29) Aft, R. L.; Lewis, J. S.; Zhang, F.; Kim, J.; Welch, M. J. *Cancer Res.* **2003**, *63* (17), 5496.
(30) Xue, Z.-M.; Tian, Y.-P.; Wang, D.; Jiang, M.-H. *Dalton Trans.* **2003**, 1373.
(31) Cowley, A. R.; Davis, J.; Dilworth, J. R.; Donnelly, P. S.; Dobson, R.; Nightingale, A.; Peach, J. M.; Shore, B.; Kerr, D.; Seymour, L. *Chem. Commun.* **2005**, 845.
(32) Bahr, G.; Schleitzer, G. *Z. Anorg. Allg. Chem.* **1955**, *280*, 161.
(33) West, D. X.; Liberta, A. E.; Padhye, S. B.; Chikate, R. C.; Sonawane, P. B.; Kumbhar, A. S.; Yerande, R. G. *Coord. Chem. Rev.* **1993**, *123* (1−2), 49.
(34) Lim, J. K.; Mathias, C. J.; Green, M. A. *J. Med. Chem.* **1997**, *40* (1), 132.
(35) Hall, I. H.; Lackey, C. B.; Kistler, T. D.; Ives, J. S.; Beraldo, H.; Ackerman, L. J.; West, D. X. *Arch. Pharm.* **2000**, *333* (7), 217.
(36) Ackerman, L. J.; West, D. X.; Mathias, C. J.; Green, M. A. *Nucl. Med. Biol.* **1999**, *26* (5), 551.
(37) Beraldo, H.; West, D. X. *Transition Met. Chem.* **1997**, *22* (3), 294.
(38) Christlieb, M.; Dilworth, J. R. *Chem.—Eur. J.* **2006**, *12*, 6194.

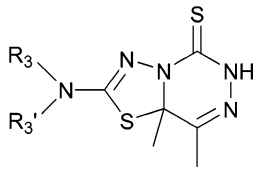

Figure 3. Bicycle formed upon heating bis(thiosemicarbazone) proligands synthesized from 2,3-butadione, where, for example, R_3 = Me and $R_3' = Ph$.

separation difficult, and obtaining sufficient pure material to characterize the ligands is challenging. Christlieb et al.[39] have recently noted that the chemistry can be complicated further by the potential of the bis(thiosemicarbazone) proligands to eliminate a terminal amino group upon heating in ethanol with a glacial acetic acid catalyst, forming highly colored bicyclic systems as shown in Figure 3. Facile elimination and cyclization occurs when R_3 = Me, R_3' = Ph, and many other ring-closure reactions are possible.[40−42] Reaction conditions must be carefully controlled in order to minimize these side reactions.

Recent experimental[13] and computational[43] results suggest that electron-donating substituents should be placed at R_1 and R_2 positions in order to lower the one-electron-reduction potential of the copper(II) complexes to more negative values, potentially conferring hypoxia selectivity. Therefore, all compounds synthesized are derived from 2,3-butadione, which provides electron-donating methyl groups on the backbone R_1 and R_2 positions.

The synthesis of zinc(II) bis(thiosemicarbazonato) complexes was achieved in three steps, as shown in Scheme 1. Compounds **1**−**17** have been characterized by NMR spectroscopy, mass spectrometry, reverse-phase high-performance liquid chromatography (HPLC), and microanalysis. Various 2D NMR techniques including COSY, HMQC, and HMBC were used, where further information was required in order to assign the NMR spectra. The electronic absorption and fluorescence emission spectra of the zinc(II) complexes **12**−**17** have also been recorded.

4-*N*-Allyl-3-thiosemicarbazide (**1**) was obtained in 55% yield from a procedure based on that described by Scovill.[44] Other 4-N-substituted 3-thiosemicarbazides were obtained from commercial sources and used as received. The allyl group was used to introduce the future possibility of using either Grubbs type metathesis or 1,3-dipolar additions for coupling bis(thiosemicarbazonato) complexes to biomolecules.[45,46]

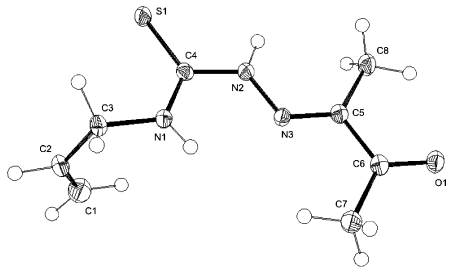

Figure 4. ORTEP[47] representation of **5**, with thermal ellipsoids shown at 50% probability.

Isolation of the monoketothiosemicarbazone intermediates, **2**−**5**, is the key step in the synthesis of unsymmetrical bis(thiosemicarbazone) proligands, where $R_3 \neq R_4$. Compounds **4** and **5** are described here for the first time. The reaction is driven by precipitation of the products from the aqueous reaction mixture and proceeds rapidly at 0 °C using 1.2 equiv of 2,3-butadione and a few drops of concentrated HCl to catalyze imine condensation (Scheme 1, step a). The monoketothiosemicarbazones are formed in the absence of acid but only in very low yields (<10% in 24 h). Excess diketone is required to limit the formation of symmetric bis(thiosemicarbazone) byproducts. Integration of the ^{1}H NMR signals indicates that the isolated solids usually contained <5% bis(thiosemicarbazone) impurity. Interestingly, it was found that increasing the size of the terminal amine substituent, R_3, decreases the amount of symmetric bis(thiosemicarbazone) byproduct formed. Further purification can be achieved by repeated recrystallization from hot aqueous ethanol. It is essential that the monoketothiosemicarbazones are purified before they are used in reaction step b because the symmetric bis(thiosemicarbazone) byproducts can be extremely difficult to separate from the desired unsymmetrical proligands.

The X-ray crystal structure of compound **5** is shown in Figure 4. Crystallographic data for all structures solved are given in Table 1. All of the non-hydrogen atoms are approximately coplanar with the exception of the C1 and C2 carbon atoms of the allyl group, which lie perpendicular to the best plane of the molecule. The three nitrogen atoms are in a trigonal-planar geometry, indicating sp^2 hybridization, and the *r*(C−N), *r*(C═S), and *r*(N−N) bonds are all intermediate in length between average distances expected for single and double bonds.[48] This structure is consistent with the extensive delocalization of the electron density expected for conjugated thiosemicarbazone systems.

Once the monoketothiosemicarbazones were available, the unsymmetrical proligands were synthesized (Scheme 1, step b). This reaction was found to be highly sensitive to the conditions used and to the rate and order of the addition of the reactants. General procedure B, given in the Experimental Section, details the method found to be optimal in both synthetic yield and minimization of the formation of byproducts. Lower temperatures with extended reaction times are preferable. The new compounds **6**−**11** were isolated in high

(39) Christlieb, M.; Claughton, H. J.; Cowley, A. R.; Heslop, J. M.; Dilworth, J. R. *Transition Met. Chem.* **2006**, *31* (1), 88.
(40) Karabatsos, G. J.; Vane, F. M.; Taller, R. A.; Hsi, N. *J. Am. Chem. Soc.* **1964**, *86* (16), 3351.
(41) Alsop, L.; Cowley, A. R.; Dilworth, J. R.; Donnelly, P. S.; Peach, J. M.; Rider, J. T. *Inorg. Chim. Acta* **2005**, *358* (9), 2770.
(42) Casas, J. S.; Castano, M. V.; Castellano, E. E.; Ellena, J.; Garcia-Tasende, M. S.; Gato, A.; Sanchez, A.; Sanjuan, L. M.; Sordo, J. *Inorg. Chem.* **2002**, *41* (6), 1550.
(43) Holland, J. P.; Green, J. C.; Dilworth, J. R. *Dalton Trans.* **2006**, 783.
(44) Scovill, J. P. *Phosphorus, Sulfur Silicon Relat. Elem.* **1991**, *60*, 15.
(45) Grubbs, R. H. *Tetrahedron* **2004**, *60* (34), 7117.
(46) Kolb, H. C.; Sharpless, K. B. *Drug Discovery Today* **2003**, *8* (24), 1128.
(47) Farrugia, L. J. *J. Appl. Crystallogr.* **1997**, *30* (5, part 1), 565.
(48) Allen, F. H.; Kennard, O.; Watson, D. G.; Brammer, L.; Orpen, A. G.; Taylor, R. *J. Chem. Soc., Perkin Trans. 2* **1987**, S1.

Table 1. Crystallographic Data for Compounds **5**, **11**, **12**, and **17**

crystal identification	**5**	H_2ATSE/Allyl, **11**	ZnATSM/A, **12**	ZnATSE/Allyl, **17**
chemical formula	$C_8H_{13}N_3OS$	$C_{11}H_{20}N_6S_2$	$C_7H_{13}N_7S_2Zn$	$C_{12}H_{22}N_6OS_2Zn$
fw	199.28	300.12	324.77	395.86
T/K	150	150	150	150
λ/Å	0.710 73	0.710 73	0.845 70[a]	0.710 73
cryst syst	monoclinic	monoclinic	orthorhombic	monoclinic
space group	$P2_1/n$	$P2_1/n$	$Pna2_1$	$P2_1/n$
a/Å	6.8603(2)	9.7912(2)	9.8643(14)	7.4508(2)
b/Å	17.3868(4)	14.1514(4)	14.627(2)	14.7225(3)
c/Å	8.5281(2)	9.4058(2)	17.117(2)	16.3562(3)
α/deg	90	90	90	90
β/deg	90.1257(11)	116.4334(16)	90	99.5855(8)
γ/deg	90	90	90	90
V/Å^3	1017.22(4)	1167.01(5)	2469.7(6)	1769.13(7)
Z	4	2	8	4
D_c/g cm^{-3}	1.301	1.300	1.747	1.486
abs coeff, μ/mm^{-1}	0.284	0.429	2.316	1.634
F(000)	424	488	1328	824
size/mm	0.14 × 0.18 × 0.24	0.14 × 0.24 × 0.26	0.089 × 0.11 × 0.168	0.10 × 0.10 × 0.32
cryst description	colorless block	colorless block	yellow needle	yellow prism
θ range collected/deg	$5.0 \le \theta \le 27.5$	$5.0 \le \theta \le 27.5$	$1.0 \le \theta \le 32.0$	$5.0 \le \theta \le 27.5$
index ranges, hkl	$-8 \le h \le 8$, $0 \le k \le 22$, $0 \le l \le 11$	$-12 \le h \le 11$, $0 \le k \le 18$, $0 \le l \le 12$	$0 \le h \le 12$, $0 \le k \le 18$, $-21 \le l \le 20$	$-9 \le h \le 9$, $0 \le k \le 19$, $0 \le l \le 21$
measd reflns	11 561	10 138	16 526	18 591
unique reflns	2384	2764	4611	4164
R_{int}	0.054	0.029	0.063	0.063
obsd reflns, n [$I > n\sigma(I)$]	1562	2141	2920	2537
transm coeff (min, max)	0.93, 0.96	0.89, 0.94	1.00, 1.00	0.59, 0.85
param refined	126	153	307	258
R or R1 (obsd reflns)	$R = 0.0345$	$R = 0.0400$	0.0380	$R = 0.0386$
wR or R2 (all data)	$wR = 0.0381$	$wR = 0.0472$	0.0433	$wR = 0.0453$
GOF	1.1063	1.0685	1.1044	1.1280
residual electron (min, max)/e Å^{-3}	−0.28, 0.29	−0.41, 0.85	−0.45, 0.97	−0.63, 0.45

[a] Synchrotron radiation source.

yields as cream/white powders. During the optimization of the procedure, it was discovered that compounds with a more yellow appearance were obtained with higher reaction temperatures. Reverse-phase HPLC chromatograms of these yellow samples often showed the presence of up to three minor species in addition to the desired proligands. These peaks were assigned by comparison of their retention times to the monoketothiosemicarbazone, the symmetric bis(thiosemicarbazone) byproduct, and probably a bicyclic system similar to that shown in Figure 3, which is likely to be responsible for the color change. Analytically pure samples of compounds **6**−**11** were obtained by repeated washing with warm dimethyl sulfoxide (DMSO)/water. However, excess heating led to decomposition of the proligands.

The X-ray crystal structure of compound **11** is shown in Figure 5. The unsymmetrical bis(thiosemicarbazone) lies on a crystallographic center of inversion, which requires that the terminal ethyl and allyl groups are substitutionally disordered. For clarity, only one of each substituent is shown in Figure 5. This disorder is also consistent with the presence of two symmetric bis(thiosemicarbazone) products. However, all other characterization data indicate that only the unsymmetrical proligand is present. Therefore, the disorder within the crystal structure is assigned to different orientations of the proligand. With the exception of the terminal allyl and ethyl groups, all heavy atoms are found to be coplanar. The allyl and ethyl groups lie perpendicular to the best plane of the molecule and have antiparallel orientation with respect to each other. The carbon−carbon bond length between C5 and C6 is 1.478(3) Å, which is exactly the same as the average bond length expected for a single bond between two sp^2-hybridized carbon atoms.[48] Other bond lengths are indicative of a conjugated system.

Zinc(II) complexes **12**−**17** were prepared by the reaction of the H_2ATSR_3/R_4 proligands, **6**−**11**, with zinc(II) diacetate dihydrate, $Zn(OAc)_2{\cdot}2H_2O$, under reflux in methanol for 4 h. No additional base was required. The neutral zinc(II) complexes precipitated from the reaction mixture and were readily isolated by filtration. X-ray crystal structures of two zinc complexes, **12** and **17**, are shown in Figures 6 and 7, respectively. In both complexes, the zinc(II) ion has a distorted square-pyramidal geometry. The axial coordination site is occupied by the terminal amino group from a second molecule of ZnATSM/A in complex **12**, whereas in **17**, the oxygen atom from a molecule of methanol is coordinated to the zinc(II) ion. In complex **12**, the zinc(II) ion is displaced from the best plane of the bis(thiosemicarbazonato) donor atoms, toward the N2_7 atom of a second molecule of ZnATSM/A by approximately 0.47 Å. The backbone carbon−carbon bond length between C3 and C4 is 1.481(11) Å. In complex **17**, disorder similar to that displayed in compound **11** was observed for the allyl and ethyl groups. The zinc(II) ion is displaced from the best plane of the donor atoms toward the oxygen atom of the methanol ligand by 0.43 Å. The backbone carbon−carbon bond length between C5 and C6 is 1.498(5) Å, an increase of 0.02 Å from the proligand

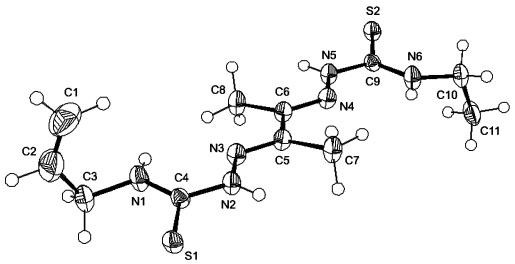

Figure 5. ORTEP representation of **11**, with thermal ellipsoids shown at 50% probability. The crystal structure contains 1 equiv of DMSO, which forms a hydrogen bond with one of the terminal NH groups, N1 or N6. The DMSO molecule has been removed for clarity.

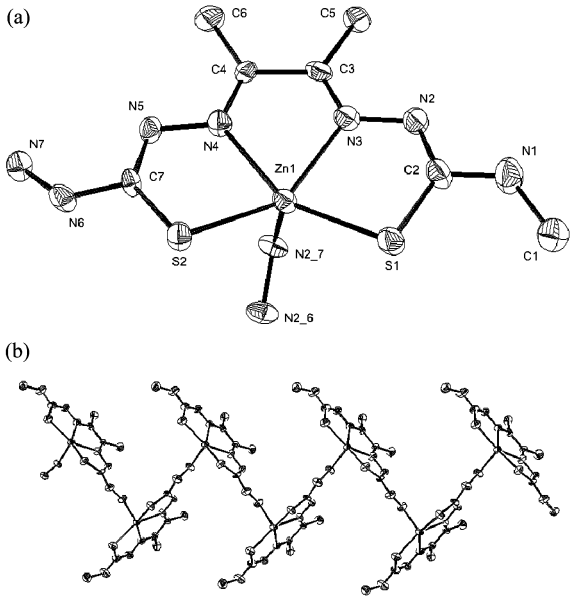

Figure 6. (a) ORTEP representation of **12**. The N2_6 and N2_7 atoms are from a second molecule and are shown to highlight the distorted square-pyramidal geometry of the zinc(II) ion. Geometrically positioned hydrogen atoms have been excluded for clarity, and thermal ellipsoids are shown at 50% probability. (b) Crystal packing of the complex.

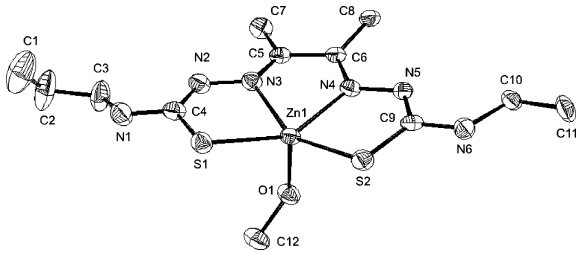

Figure 7. ORTEP representation of **17**, with thermal ellipsoids shown at 50% probability.

11. All characterization data are consistent with the proposed structures for complexes **12**−**17**.

Copper Complexes. Copper(II) complexes **18** and **19** were synthesized in high yield by the reaction of proligands **10** and **11** with copper(II) diacetate monohydrate, $Cu(OAc)_2 \cdot H_2O$, under reflux in methanol for 4 h (Figure 8). Microanalysis and high-resolution mass spectrometry were found to be consistent with the proposed complexes, and both **18** and **19** give a single peak by reverse-phase HPLC.

The simulated and experimental electron paramagnetic resonance (EPR) spectrum of **19**, recorded in *N*,*N*-dimethylformamide (DMF) at room temperature, is shown in Figure 9. The solution-phase spectrum is essentially identical with that of the hypoxia-selective complex diacetylbis(4-*N*-methyl-3-thiosemicarbazonato)copper(II), CuATSM (Figure 8).[49,50] Complex **19** exhibits copper hyperfine splittings of 93 G with nitrogen superhyperfine lines in a 1:2:3:2:1 ratio ($A_N = 16.5$ G) and $g_{iso} = 2.059$. This indicates that the two nitrogen donor atoms are electronically equivalent. The spectrum was simulated with EasySpin[51] using the fast-motion regime. The Kivelson formula was used to describe m_I-dependent Lorentzian line broadening (eq 1). From the best fit of the simulated

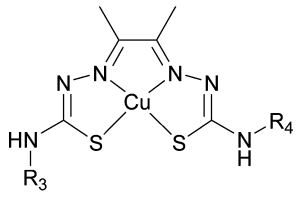

18 R_3 = allyl, R_4 = Me, 88%
19 R_3 = allyl, R_4 = Et, 94%

Figure 8. Copper(II) complexes synthesized by the reaction of proligands **10** and **11** with $Cu(OAc)_2 \cdot H_2O$ in methanol. For CuATSM, $R_3 = R_4 =$ Me.

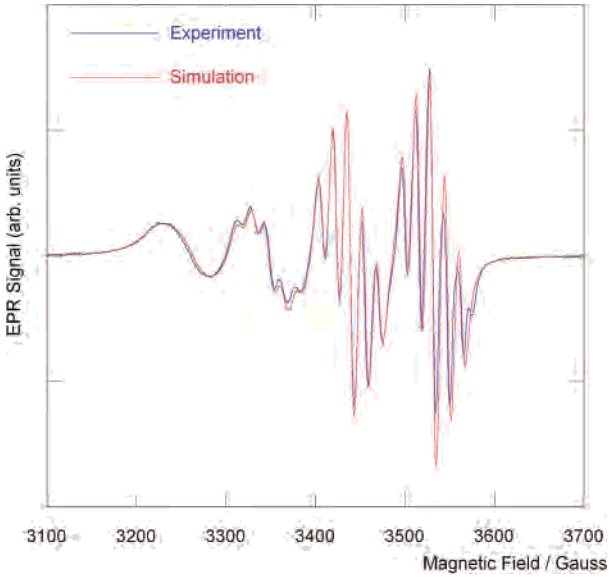

Figure 9. Solution-phase experimental (blue) and simulated (red) EPR spectrum of complex **19** in anhydrous DMF at room temperature.

$$\Gamma(m_I) = a + bm_I + cm_I^2 \qquad (1)$$

spectrum, the optimized line-broadening parameters were found to be $a = 2.10$, $b = 1.16$, and $c = 0.49$. In the simulation, it was assumed that the copper ion was copper-63. However, the copper acetate used was a mixture of copper-63 and copper-65 in natural abundance (69.17 and 30.83%, respectively).[52] These two isotopes have slightly different nuclear magnetic moments of 2.22 and 2.38,

(49) Warren, L. E.; Horner, S. M.; Hatfield, W. E. *J. Am. Chem. Soc.* **1972**, *94* (18), 6392.
(50) West, D. X.; Ives, J. S.; Bain, G. A.; Liberta, A. E.; Valdes-Martinez, J.; Ebert, K. H.; Hernandez-Ortega, S. *Polyhedron* **1997**, *16* (11), 1895.
(51) Stoll, S.; Schweiger, A. *J. Magn. Res.* **2006**, *178* (1), 42.
(52) Rosman, K. J. R.; Taylor, P. D. P. *Pure Appl. Chem.* **1998**, *70* (1), 217.

respectively, which may account for minor differences observed between the experimental and simulated EPR spectra.

Attempts to synthesize and isolate copper(II) complexes of proligands **6**−**9** were unsuccessful. Changing the copper(II) salt used (chloride, acetate, nitrate, and tetrafluoroborate), reaction solvent (methanol, ethanol, tetrahydrofuran, acetonitrile, DMSO, and DMF), time scale, and temperature made little difference. In all cases, mass spectrometry indicated that the desired complexes were present. However, additional intractable copper species were also observed, and reverse-phase HPLC chromatograms of reaction mixtures and isolated solids typically contained several unidentified peaks. The pendent amino group appears to complicate the copper(II) complexation reaction, possibly by competing with other nitrogen and sulfur atoms as a ligand or by participating in redox chemistry. It is also possible that the complexes may decompose on the HPLC column.

The fact that $Cu^{II}ATSR_3$/A complexes could not be isolated at this stage is not detrimental to the design or synthesis of more elaborate systems. On a radiopharmaceutical scale ($<10^{-8}$ mol dm^{-3} concentration of copper radionuclide), complex, multistage synthesis is undesirable.[2] Very low concentrations mean that bimolecular reaction rates will be extremely slow, which potentially restricts the synthesis of bioconjugated systems. In addition, most coupling reactions require the use of organic solvents. The presence of water may inhibit coupling reactions, for example, imine condensation. Since the copper radionuclides are obtained in aqueous solution, this represents a significant obstacle to performing coupling reactions postradiolabeling. Therefore, the preferred method is to insert the copper radionuclide in the final step as described in the Copper-64 Radiolabeling and Transmetalation sections.

Electrochemistry. The mechanism of hypoxia selectivity of copper(II) bis(thiosemicarbazonato) complexes is thought to involve an initial intracellular reduction to give the copper(I) anion, possibly followed by protonation or ligand dissociation.[43] Blower et al. conducted extensive structure−activity relationship studies and found that hypoxia selectivity strongly correlated with both the copper(II/I) redox potential and the alkyl substitution pattern on the ligand backbone.[13] Experimental and computational studies suggest that more electron-donating substituents on the ligand backbone (R_1 and R_2) lower the copper(II/I) reduction potential. In comparison, the terminal amine substituents (R_3 and R_4) have a relatively minor influence on the electron density at the copper(II) center. Therefore, one-electron-reduction potentials of complexes **18** and **19** are expected to be similar to that of $Cu^{II}ATSM$, which has a reversible copper(II/I) redox couple at $E_{1/2}$(DMF) = −0.62 V vs a saturated calomel reference electrode (SCE).[53]

Electrochemical data for copper(II) complexes **18** and **19** are given in Table 2, and the cyclic voltammogram of **19** recorded with a platinum working electrode at a potential scan rate of 150 mV s^{-1} in anhydrous DMF is shown in Figure 10. In light of their structural similarity with CuATSM, as expected, complexes **18** and **19** exhibit a quasi-reversible one-electron-reduction process assigned to the metal-centered copper(II/I) redox couple at $E_{1/2}$(SCE) = −0.632 and −0.636 V, respectively.[43] These values are within the biological window for hypoxia selectivity and demonstrate that bis(thiosemicarbazonato) complexes may be functionalized at the terminal amino positions without inducing large changes in the redox potential.[13] As a result, the mechanism of trapping within hypoxic tissue is expected to be similar to that of CuATSM. However, the behavior of a compound in vivo is dependent upon many factors. Although the redox chemistry of copper(II) bis(thiosemicarbazonato) complexes may be controlled, functionalization is likely to induce large changes in polarity, lipophilicity, and pK_a. This may have dramatic effects on the biodistribution, cell uptake, and intracellular localization of a potential radiopharmaceutical.

Both **18** and **19** exhibit a one-electron oxidation at $E_{1/2}$(SCE) = +0.730 and +0.724 V, respectively. For complex **19**, this oxidation process is reversible but from, the peak current ratio, $|i_{pa}|/|i_{pc}|$, of 1.571, appears quasi-reversible for complex **18**. This is consistent with previous electrochemical observations on CuATSM, which partially

Table 2. Electrochemical Data for Copper Complexes **18** and **19** at 150 mV s^{-1}

	ΔE_p/V[a]	$E_{1/2}$(SCE)/V	$\lvert i_{pa}\rvert/\lvert i_{pc}\rvert$[b]
	Copper(II/I)		
18	0.131	−0.631	0.897
19	0.152	−0.636	0.976
	Copper(III/II)		
18	0.074	0.730	1.571
19	0.091	0.724	1.129

[a] The difference in the peak potentials is given by $\Delta E_p = E_{pa} - E_{pc}$, where the subscripts pa and pc refer to the anodic and cathodic peaks, respectively. [b] Ratio of the peak currents.

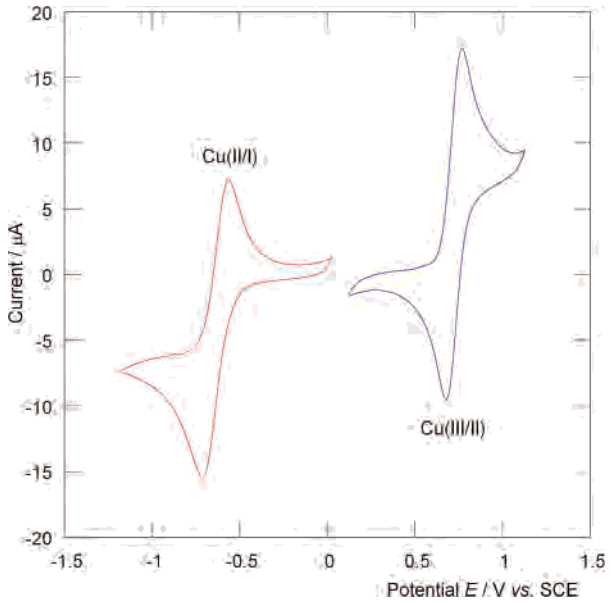

Figure 10. Cyclic voltammogram of CuATSE/Allyl (**19**) at 150 mV s^{-1} in anhydrous, degassed DMF: (red) copper(II/I) redox wave; (blue) copper(III/II) redox wave.

(53) Cowley, A. R.; Dilworth, J. R.; Donnelly, P. S.; Gee, A. D.; Heslop, J. M. *Dalton Trans.* **2004**, 2404.

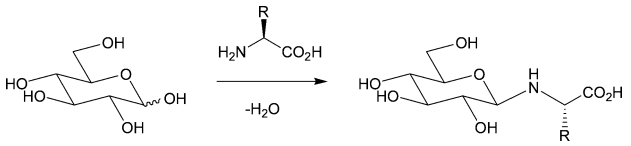

Figure 11. Condensation of an amino acid with α,β-D-glucose, forming the *N*-glucosylamine intermediate.

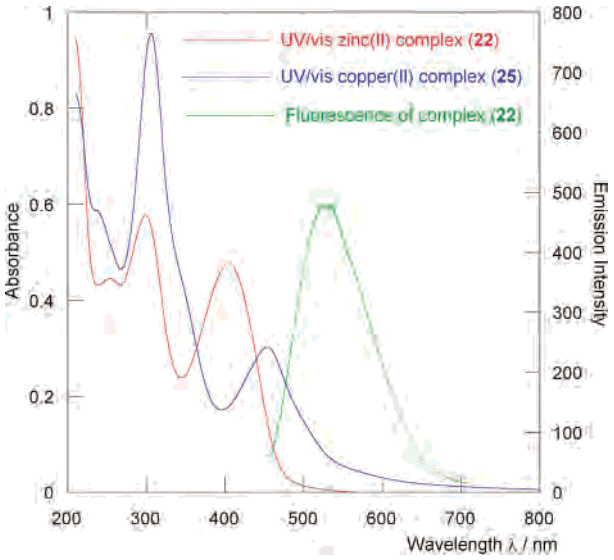

Figure 12. Experimental UV/vis absorption spectrum and fluorescence emission spectrum (λ_{ex} = 380 nm) of 0.05 mmol dm^{-3} **22** in water and the resulting UV/vis spectrum after the addition of 1 equiv of $Cu(OAc)_2$(aq) (0.01 mol dm^{-3}) to give **25**.

decomposes upon oxidation in acetonitrile.[49] The oxidation process has previously been assigned to the copper(III/II) redox couple. However, at present, the nature of the oxidized complex is unknown, and it is possible that the electron is removed from either the copper(II) ion or the ligand. Previous DFT calculations suggest that the highest occupied molecular orbital (HOMO) resides in the β-spin orbital manifold and has ligand-based π character.[43]

Glucose Functionalization. The terminal amino group of complexes **12**−**15** may be viewed as a reactive group that can be used to functionalize the bis(thiosemicarbazonato) complex with a BAM. To demonstrate that these complexes can be used in the bioconjugation methodology outlined above, the reaction with α,β-D-glucose was investigated. Nonenzymatic reactions between amino acids and saccharides are ubiquitous in nature and were first identified by Maillard in 1912.[54] The initial step in the Maillard reaction network usually involves the condensation of an amine with the carbonyl group of a reducing sugar, forming *N*-glycosylamine intermediates (Figure 11).[55−57] These intermediates then react via Amadori rearrangements,[58] forming a complicated and diverse network of chemistry that has been well characterized and represents important areas in both food science and medical research into aging.[56]

Scheme 2 shows the coupling reaction used for the synthesis of three glucose-functionalized zinc(II) complexes, **20**−**22**. The coupling reaction was conducted in methanol under reflux using 1 drop of a 10% HCl(aq) acid catalyst. As the reaction proceeded, the yellow suspension of $ZnATSR_3$/A dissolved and a clear deep-orange/red solution formed. The coupled complexes were precipitated from the reaction mixture by the slow addition of diethyl ether and were characterized by ^{1}H and ^{13}C{^{1}H} NMR spectroscopy, high-resolution mass spectrometry, reverse-phase HPLC, UV/vis, and fluorescence emission spectroscopy. Complexes **20**−**22** were formed in high yield and were found to be highly soluble in water, resulting in bright-yellow solutions. In contrast, complexes **12**−**17** are insoluble in water. Both HPLC and NMR spectroscopy indicate that only one major species is present in solution.

The conformation and connectivity of the saccharide group in complexes **20**−**22** were confirmed by ^{1}H, ^{13}C{^{1}H}, COSY, and HMQC NMR spectroscopy. The 500-MHz ^{1}H NMR spectrum of **22** in methanol-d_4 shows signals with the expected coupling pattern for the allyl group (δ 5.93, 5.20, and 5.08 ppm) and two singlets for the methyl groups of the bis(thiosemicarbazonato) backbone (δ 2.29 and 2.27 ppm). Resonances for the *N*-glucosylamino functional group occur between δ 3.20 and 4.00 ppm. The anomeric C1 proton (H1) is identified as a doublet at δ 4.00 ppm, and the magnitude of the coupling constant ($^3J_{1,2}$ = 8.9 Hz) indicates that the proton is axial with respect to the ring. Therefore, the major species formed is the β-anomer, where the sterically large bis(thiosemicarbazonato) group lies in the equatorial ring position. The H2, H3, and H4 protons were identified from the 2D COSY NMR cross peaks starting from the anomeric H1 resonance. Each peak shows the expected coupling pattern. The peak for H5 lies underneath the residual methanol solvent peak at δ 3.31 ppm and shows a cross peak in the COSY spectrum with both of the protons H6a and H6b at δ 3.87 and 3.68 ppm, respectively. The ^{13}C{^{1}H} NMR spectrum was assigned using the HMQC experiment, and the results are consistent with the assignments for other *N*-glucosylamine systems.[59] Despite repeated attempts to purify compounds **20**−**22**, the ^{1}H NMR spectra indicate the presence of <5% free α,β-D-glucose by integration, which most likely accounts for inaccuracies observed in the microanalyses of these compounds. The zinc(II) glucose conjugates **20** and **21** exhibit NMR spectra very similar to that of complex **22**.

Aqueous solutions of copper(II) complexes **23**−**25** were made via transmetalation in water by mixing 1 equiv of copper(II) acetate, $Cu(OAc)_2$(aq), with the corresponding zinc(II) complexes, **20**−**22**, at room temperature. Reverse-phase HPLC can resolve the zinc(II) and copper(II) bis(thiosemicarbazonato) complexes and shows one major peak for each zinc(II) complex. For complex **22**, the peak for the zinc(II) species had a retention time R_t = 5.63 min. This peak disappeared upon the addition of 1 equiv of copper acetate, and a new peak at slightly longer retention time

(54) Maillard, L. C. *C. R. Acad. Sci., Ser. 2* **1912**, *154*, 66.
(55) Ledl, F.; Schleicher, E. *Angew. Chem.* **1990**, *102* (6), 597.
(56) Gerrard, J. A. *Aust. J. Chem.* **2002**, *55* (5), 299.
(57) Davidek, T.; Clety, N.; Aubin, S.; Blank, I. *J. Agric. Food Chem.* **2002**, *50* (19), 5472.
(58) Turner, J. J.; Wilschut, N.; Overkleeft, H. S.; Klaffke, W.; Van Der Marel, G. A.; Van Boom, J. H. *Tetrahedron Lett.* **1999**, *40* (38), 7039.
(59) Lederer, M. O.; Dreisbusch, C. M.; Bundschuh, R. M. *Carbohydr. Res.* **1997**, *301* (3−4), 111.

Table 3. UV/Vis and Fluorescence Spectroscopy Data for All Zinc(II) and Copper(II) Complexes

	UV/vis				fluorescence $\lambda_{ex} = 380$ nm		
	$\lambda_{max}(1)$/nm	$\epsilon(\lambda_1)$/mol^{-1} dm^3 cm^{-1}	$\lambda_{max}(2)$/nm	$\epsilon(\lambda_2)$/mol^{-1} dm^3 cm^{-1}	λ_{em}/nm	intensity, I_{max}	quantum yield, Φ_f
12	431	11 705 ± 217	314	10 825 ± 212	527	529	0.0201[b]
13[a]	433	12 337 ± 235			530	525	0.0201[b]
14	439	13 919 ± 290	326	11 981 ± 220	547	553	0.0061[b]
15	433	11 416 ± 143	314	10 424 ± 140	530	547	0.0081[b]
16	435	13 264 ± 721	315	13 512 ± 694	530	1012	0.0238[b]
17	433	8579 ± 140	314	8361 ± 93	531	696	0.0297[b]
18	476	5172 ± 266	314	15 443 ± 705			
19	477	5627 ± 282	315	16 693 ± 772			
20	403	8434 ± 414	296	9899 ± 468	529	574	0.0091[c]
21	404	8866 ± 533	296	9670 ± 439	531	660	0.0135[c]
22	405	9531 ± 470	298	10 801 ± 507	529	629	
23	452	5229 ± 281	305	17 356 ± 486			
24	457	5929 ± 196	309	15 976 ± 525			
25	454	5777 ± 290	306	19 350 ± 624			

[a] The second UV/vis peak for complex **13** is obscured by solvent absorption. [b] Measured in DMSO. [c] Measured in water relative to $[Ru(byp)_3][PF_6]_2$; $\Phi_f = 0.042$ in water.

Scheme 2. General Reaction Scheme for the Synthesis of Glucose-Functionalized Zinc(II) and Copper(II) Bis(thiosemicarbazonato) Complexes[a]

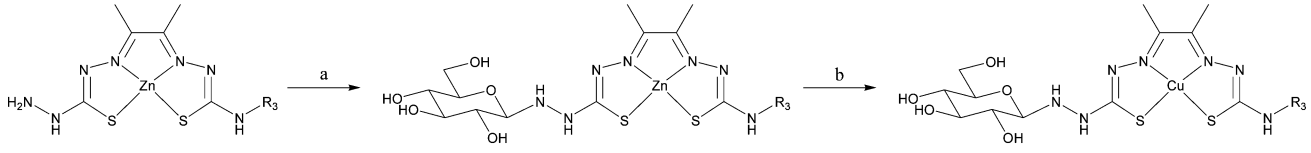

12 R_3 = Me, 97%
13 R_3 = Et, 95%
15 R_3 = allyl, 83%

20 ZnATSM/A-Glc, R_3 = Me, 84%
21 ZnATSE/A-Glc, R_3 = Et, 93%
22 ZnATSAllyl/A-Glc, R_3 = allyl, 88%

23 CuATSM/A-Glc, R_3 = Me,
24 CuATSE/A-Glc, R_3 = Et,
25 CuATSAllyl/A-Glc, R_3 = allyl,

[a] (a) α,β-D-Glucose (1 equiv), 10% HCl(aq) catalyst, methanol, reflux, 12 h. (b) Transmetalation reactions: aqueous solutions of the corresponding zinc(II) complex, **20**−**22**, were mixed with an aqueous solution of $Cu(OAc)_2{\cdot}H_2O$ (1 equiv), stir, and rtp, <1 min.

developed (R_t = 6.70 min). This demonstrates that the transmetalation reaction occurs cleanly to give a single copper(II) species (**25**). Short retention times indicate that the complexes are hydrophilic, which suggests that transmetalation does not induce fragmentation or loss of the polyhydroxyl *N*-glucosylamino functional group. The difference in the retention times between zinc(II) and copper(II) bis(thiosemicarbazonato) complexes, **16**−**25**, is likely due to a change in the geometry induced by the coordination of a solvent molecule in the axial site of the zinc(II) complexes. Crystal structures of zinc(II) bis(thiosemicarbazonato) complexes often show a coordinated solvent molecule in the axial site (Figure 7).

High-resolution mass spectrometry showed the presence of the $\{M + H^+\}$ peak for the zinc(II) complexes **12**−**22**. However, all attempts to obtain mass spectra of complexes **23**−**25** were unsuccessful. Copper(II) bis(thiosemicarbazonato) complexes often do not give mass spectra because the parent ion may be difficult to form or may fragment under the mass spectrometry conditions. Further evidence to support the identity of the copper(II) glucose conjugates was obtained via UV/vis, fluorescence, and EPR spectroscopy. In addition, the copper-64-radiolabeled complexes of **19** and **24** have been prepared.

Figure 12 shows the electronic absorption spectrum of complex **22** in water and the change that occurs upon the addition of 1 equiv of copper(II) acetate to give complex **25**. The fluorescence emission spectrum of **22** is also shown (Figure 12). Upon the addition of copper(II) acetate, the yellow zinc(II) solution rapidly changes color to give a red/brown solution and the UV/vis spectrum becomes qualitatively similar to that of CuATSM (Figure 17, vide infra).[49] Experimental UV/vis and fluorescence data for complexes **12**−**25** are given in Table 3. Parts a and b of Figure 13 show the change in the UV/vis and fluorescence emission spectra of complex **22** (0.05 mmol dm^{-3}) in water upon titration with 5.0-μL aliquots of $Cu(OAc)_2$(aq) (2.0 mmol dm^{-3}), respectively. The final spectra presented were recorded after the addition of 1.06 equiv of copper(II) acetate. The UV/vis spectra show well-defined isosbestic points at 443 and 363 nm. This further demonstrates that the transmetalation reaction proceeds cleanly in an aqueous solution. The fluorescence emission intensity decreases linearly upon titration with copper(II) acetate because of the decreased concentration of zinc(II) complex **22**. This is consistent with the formation of a paramagnetic copper(II) complex, which provides an alternative relaxation pathway via internal conversion and vibrational relaxation for the excited states of the bis(thiosemicarbazonato) chromophore.

Fluorescence emission quantum yields (Φ_f) calculated for the excitation of a 0.025 mmol dm^{-3} zinc(II) complex at λ_{ex} = 380 nm, using $[Ru(bpy)_3][PF_6]_2$ as a reference, are also presented in Table 3.[60] The fluorescence emission spectra were measured in DMSO for compounds **12**−**17** and in water for compounds **20**−**22**. The zinc(II) bis(thiosemicarbazonato) complexes were found to be weakly fluorescent with little change in the emission wavelength or quantum yield upon changing the R_3 substituent. Complex **17** appears to have a slightly larger quantum yield of 0.03. The glucose conjugates

(60) Meech, S. R.; Phillips, D. *J. Photochem.* **1983**, *23* (3), 193.

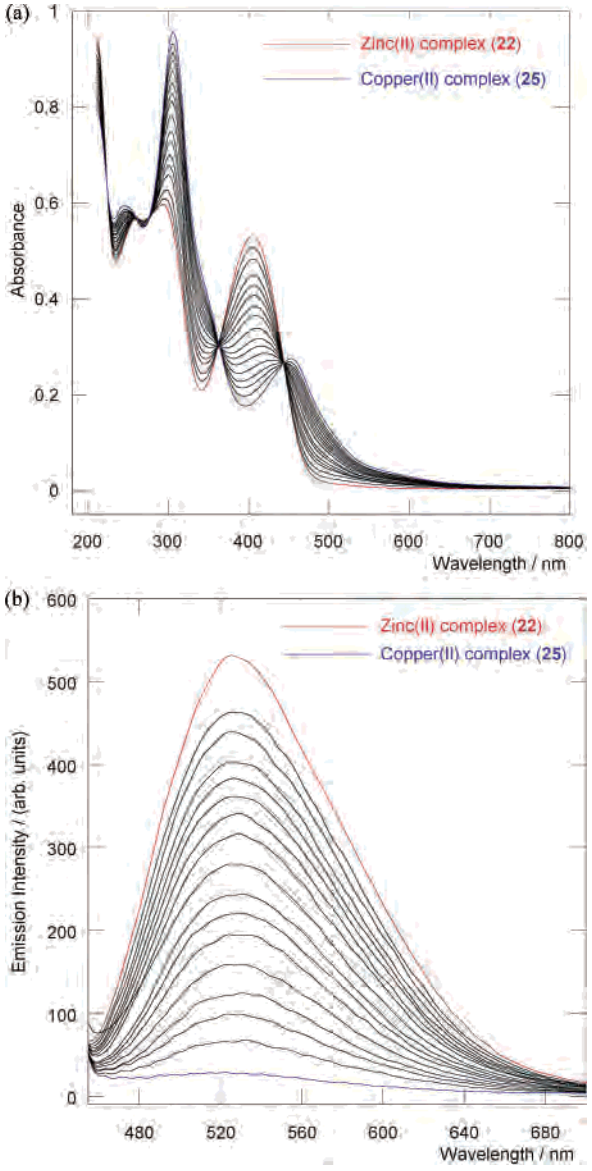

Figure 13. (a) Experimental UV/vis absorption spectra and (b) fluorescence emission spectra (λ_{ex} = 380 nm) of 3 mL of 0.05 mmol dm^{-3} **22** in water upon titration with 16 5-μL aliquots of 2.0 mmol dm^{-3} Cu(OAc)$_2$(aq) (1.06 equiv of copper) to give **25**.

remain fluorescent in water but with slightly decreased quantum yields than the complexes in DMSO.

The room-temperature EPR spectrum of complex **24** in water, prepared by mixing complex **21** with 1 equiv of Cu(OAc)$_2$ in water, is shown in Figure 14. The spectrum is very similar to that of CuATSM in DMF and of complex **19** (vide supra), indicating that the coordination environment of the copper(II) ion is the same in each complex.[49] Complex **24** exhibits copper hyperfine splittings of 89 G with nitrogen superhyperfine lines in a 1:2:3:2:1 ratio (A_N = 16.5 G) and g_{iso} = 2.065. The optimized line-broadening parameters were found to be a = 3.17, b = 2.25, and c = 0.88. All attempts to record a solution-phase EPR spectrum of CuATSM in water were unsuccessful because of the lack of solubility.

Copper-64 Radiolabeling. Copper-64-radiolabeled complexes of **19** and **24** were prepared by reacting compound **11** and complex **22** with ^{64}Cu(OAc)$_2$(aq), respectively. The

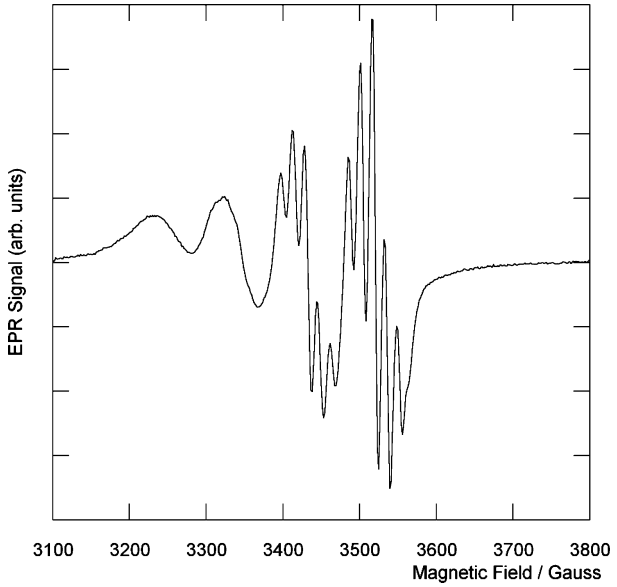

Figure 14. Experimental EPR spectrum of **24** prepared by transmetalation from **21** in water with 1 equiv of Cu(OAc)$_2$(aq).

radio-HPLC chromatograms are shown in parts a and b of Figure 15. Under the chromatographic conditions used, ^{64}Cu(OAc)$_2$(aq) was found to have a retention time R_t of 2.30 min. In each case, the reaction was followed using reverse-phase HPLC with sequential UV and radiodetection.

The radio-HPLC data show that complex **19** radiolabels cleanly to give a single copper-64 species (R_t = 16.27 min). The identity of the complex was confirmed by comparison with the UV−HPLC retention time of the isolated cold copper complex **19**. For complex **24**, two copper-64-containing species (R_t = 9.10 and 9.30 min) were resolved by radio-HPLC. The low retention times indicate that the complexes are hydrophilic, and it is likely that, in water, the *N*-glucosylamino functional group exists as a mixture of anomers. Radiolabeling of **24** was repeated on three separate occasions with the same result. These experiments also demonstrate that transmetalation is a viable method for the preparation of copper-64-radiolabeled complexes.

Preliminary cell uptake and washout studies using neutrophil cells isolated from a human blood sample with copper-64-radiolabeled complex **24** showed that, under normoxic conditions, rapid washout occurs and after three washes <1% of the copper-64 remained in the cells. This result is consistent with similar studies by Blower et al.[13] and provides evidence that copper(II) bis(thiosemicarbazonato) complexes are stable under biological conditions in vitro. Coordination and trapping by intracellular proteins would likely prevent the copper-64 from diffusing out of the cells if it were released from the bis(thiosemicarbazonato) complex. Under normoxic conditions, cellular uptake and washout is thought to establish an equilibrium. Therefore, with successive washes, leaching of the copper-64 radioactivity from the cells is expected to occur in the presence of oxygen. This indicates that complex **24** is not trapped within neutrophil cells under normoxic conditions. Investigations are underway to look at cellular uptake and trapping under hypoxic and other conditions.

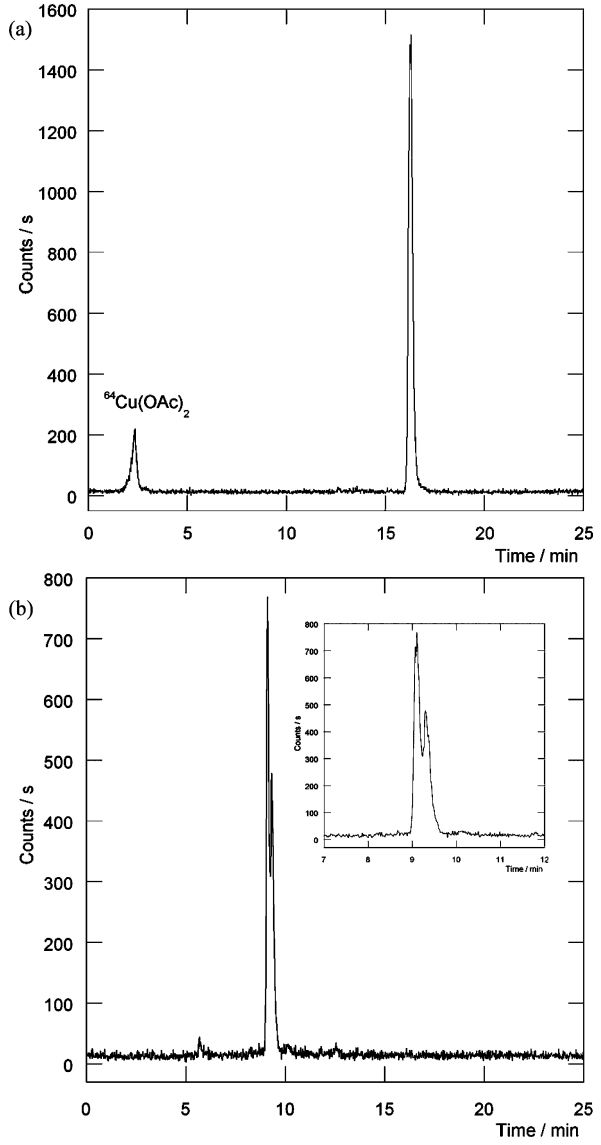

Figure 15. Radio-HPLC chromatograms of copper-64-radiolabeled complexes: (a) **19** synthesized by reaction with proligand **11**; (b) **24** prepared by transmetalation from the zinc(II) complex **21**.

Other saccharides, including mannose, galactose, 2-deoxyglucose, ribose, 2-deoxyribose, and maltose, have been successfully conjugated to complexes **12** and **13** to give water-soluble species. Characterization by HPLC and high-resolution mass spectrometry has been performed in all cases. However, structural assignment based on NMR spectroscopy has proved difficult because of the complexity of the resonances from the saccharide protons. These results will be reported in full in a future publication.

Transmetalation. The use of transmetalation was an important advance in the synthesis of copper radiopharmaceuticals. This approach was first used by Fujibayashi et al.[61] and Yokoyama et al.[62] in 1992 to radiolabel three different bis(thiosemicarbazonato) complexes with either copper-62 or copper-64, respectively.[2] However, one potential difficulty

(61) Matsumoto, K.; Fujibayashi, Y.; Arano, Y.; Wada, K.; Yokoyama, A. *Nucl. Med. Biol.* **1992**, *19* (1), 33.
(62) Saji, H.; Saiga, A.; Iida, Y.; Magata, Y.; Yokoyama, A. *J. Labelled Compd. Radiopharm.* **1993**, *33* (2), 127.

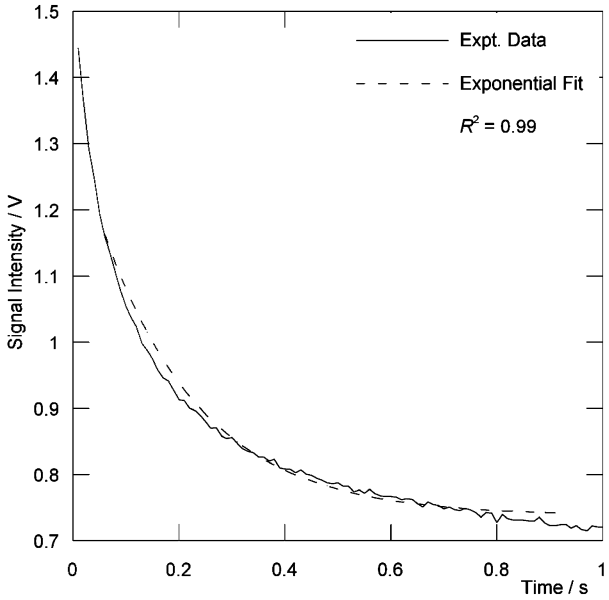

Figure 16. Pseudo-first-order decay observed for the transmetalation reaction between equal volumes of (0.1 mmol dm^{-3}) **21** and (10.0 mmol dm^{-3}) copper(II) acetate in water at 22.5 °C.

in using this method to prepare compounds with targeting groups for specific receptor sites is the removal of the large excess of zinc(II) complex from the radiolabeled sample. This is essential in order to maximize the purity of the radiopharmaceutical administered and to prevent receptor sites from being potentially saturated by the zinc(II) complex. The UV−HPLC results described here demonstrate that copper(II) bis(thiosemicarbazonato) complexes can be readily separated from their zinc(II) analogues. This extremely important observation means that copper(II)-radiolabeled complexes can be purified using simple reverse-phase radio-HPLC prior to their use as imaging agents. Therefore, the transmetalation reaction was investigated further by the use of stopped-flow kinetic experiments. The energetics of transmetalation have been modeled using DFT calculations.

Transmetalation of ZnATSE/A-Glc, **21**, to give the corresponding copper(II) complex, **24**, in water at 22.5 °C was studied by stopped-flow kinetics. The transmetalation reaction is expected to be first order with respect to both the zinc(II) bis(thiosemicarbazonato) complex and copper(II) acetate, giving an overall second-order reaction. In the preparation of radiolabeled complexes via transmetalation, there will be a large excess of the zinc(II) complex. Under these conditions, the reaction would be expected to exhibit pseudo-first-order kinetics, depending on the concentration of copper(II) in the sample. However, because of restrictions with the apparatus, the experiments had to be conducted using 10.0 mmol dm^{-3} $Cu(OAc)_2$(aq) and a 0.1 mmol dm^{-3} solution of **21** in water. The reaction was monitored by following the decrease in the signal voltage due to the formation of the copper(II) complex **24** using the emission from a blue photodiode (λ_{em} = 465−475 nm). Figure 16 shows the decay of the signal intensity as a function of time, on the formation of complex **24**. The data were averaged from five kinetic runs and fit using eq 2, where V is the

$$V_t = V_f + (V_i - V_f)e^{-k_{obs}t} \quad (2)$$

signal voltage, the subscripts i and f refer to the initial and final voltages, and t is time in seconds. The initial 50 ms and final 100 ms of data were excluded from the exponential fit to account for the apparatus dead time and the signal noise at the end of the reaction. From the exponential fit, $V_i = 1.293 \pm 0.007$ V and $V_f = 0.737 \pm 0.002$ V. The pseudo-first-order rate constant was found to be $k_{obs} = 5.34 \pm 0.14$ s^{-1} with an observed half-life $\tau_{obs} = 0.129 \pm 0.003$ s at 22.5 °C. Correcting for the change in the concentration of copper(II) acetate upon mixing gives a calculated second-order rate constant $k_2 = 1068 \pm 28$ mol^{-1} dm^3 s^{-1}. The transmetalation reaction is very rapid and, with efficient mixing, is complete within 1 s at room temperature.

Due to the large size of the glucose-conjugated species, DFT calculations were performed to model the reaction between ZnATSM and $[Cu(H_2O)_6]^{2+}$ as shown in eq 3.

$$ZnATSM + [Cu(H_2O)_6]^{2+} \rightarrow CuATSM + [Zn(H_2O)_6]^{2+} \quad (3)$$

Although the hexaaquacopper(II) species may not exist in solution because of Jahn−Teller distortion, it provides a more representative species than a free copper(II) ion for use as an energy reference in the calculations.[63]

DFT calculations were conducted using *Gaussian03*, revision C.02.[64] A further description of the methods used has been presented in ref 43. The thermodynamics of transmetalation were investigated in both the gas and solution phases using a polarizable dielectric continuum to incorporate electrostatic interactions with water as a solvation model.[65] No symmetry constraints were used. The calculated energetics are summarized in Table 4. Transmetalation is found to be spontaneous with a standard gas-phase reaction free energy of $\Delta_rG°(g) = -115$ kJ mol^{-1}. The driving force is entirely enthalpic with $\Delta_rH°(g) = -117$ kJ mol^{-1}. The change in the solvation free energy on transmetalation, $\Delta\Delta_{solv}G°$, of +10 kJ mol^{-1} means that in solution the reaction is slightly less favorable but remains spontaneous and highly exothermic with an overall $\Delta_rG°(aq) = -105$ kJ mol^{-1}.

Electronic Spectroscopy and TD−DFT Calculations. The fluorescence emission of zinc(II) bis(thiosemicarbazonato) complexes has only recently been reported, and despite over three decades of research, analysis of the electronic absorption spectrum of copper(II) complexes using DFT has not been performed.[30,31] Experimental UV/vis and fluorescence spectroscopy data for complexes **12**−**25** are summarized in Table 3 (above), and the experimental and simulated electronic absorption spectra of Cu^{II}ATSM are shown in Figures 17 and 18, respectively.

To facilitate a better understanding of the electronic transitions that occur in the copper(II) complexes, TD-DFT calculations were conducted using *Gaussian03*, revision C.02. The UV/vis spectra of all copper(II) bis(thiosemicarbazonato) complexes, including the glucose conjugates **22**−**25**, are very similar. Therefore, to simplify the calculations, the related complex, Cu^{II}ATSM, was used as a model.

Table 4. DFT-Calculated Energetics (kJ mol^{-1}) for the Transmetalation Reaction between ZnATSM and $[Cu(H_2O)_6]^{2+}$ [a]

	calcd energetics/ kJ mol^{-1}		calcd energetics/ kJ mol^{-1}
$\Delta\epsilon_{SCF}(g)$	−116	$\Delta_rG°(g)$	−115
$\Delta\epsilon_{ZPE}(g)$	−1.0	$\Delta\Delta_{solv}G°$	10
$\Delta_rH°(g)$	−117	$\Delta_rG°(aq)$	−105
$-T\Delta_rS°(g)$	2.0		

[a] $\Delta\epsilon_{SCF}$ represents the change in the electronic energy, and ZPE is the zero-point energy correction in the gas phase.

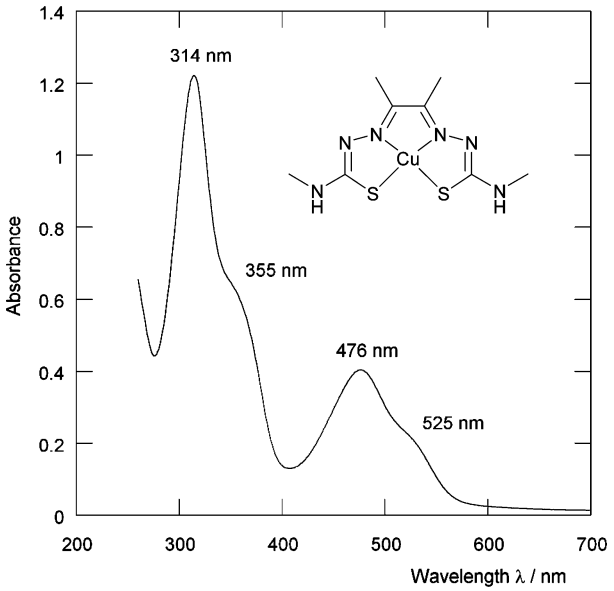

Figure 17. Experimental UV/vis absorption spectrum of 0.05 mmol dm^{-3} CuATSM (inset) in anhydrous DMF.

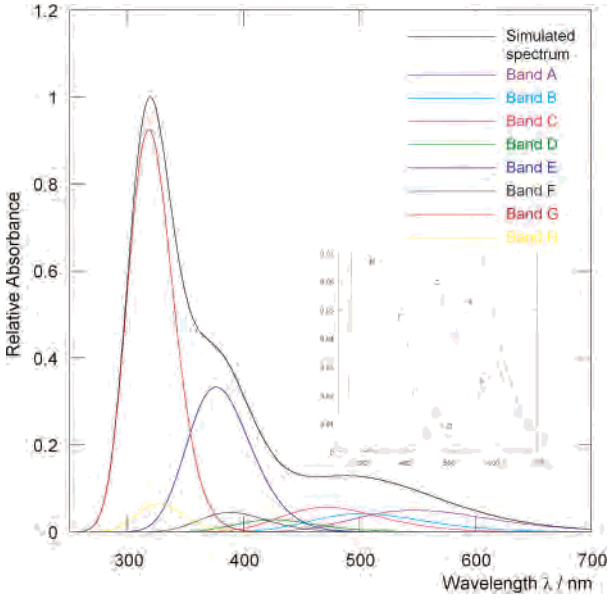

Figure 18. Simulated TD-DFT electronic absorption spectrum of Cu-ATSM in vacuo. The spectrum is modeled by eight Gaussian-shaped bands, with two major bands, G (red) and E (dark blue), and six minor bands (inset).

(63) Akesson, R.; Pettersson, L. G. M.; Sandstroem, M.; Wahlgren, U. *J. Phys. Chem.* **1992**, *96* (1), 150.
(64) *Gaussian03*. Please refer to the Supporting Information for the complete reference.
(65) Cramer, C. J.; Truhlar, D. G. *Chem. Rev.* **1999**, *99* (8), 2161.

Table 5. Excited-State and Molecular Orbital Deconvolution of the TD-DFT Simulated Electronic Absorption Spectrum[a]

absorption band[b]	excited state	oscillator strength, f	λ_{ex}(calcd)/ nm	molecular orbital contributions (%) α-spin orbitals	molecular orbital contributions (%) β-spin orbitals
A	**5**	**0.0239**	**547.9**	**HOMO → LUMO (33%)**	**HOMO → LUMO+1 (36%)**
					HOMO−5 → LUMO (19%)
B	**7**	**0.0200**	**502.1**		**HOMO−8 → LUMO (35%)**
					HOMO−5 → LUMO (23%)
					HOMO−6 → LUMO (19%)
					HOMO−12 → LUMO (13%)
C	**8**	**0.0271**	**471.1**		**HOMO−8 → LUMO (34%)**
					HOMO−12 → LUMO (29%)
					HOMO−5 → LUMO (16%)
D	9, 10, 11, 13	0.0150[c]	421.6[d]	HOMO−3 → LUMO[e]	HOMO−3 → LUMO[e]
				HOMO−4 → LUMO	HOMO−3 → LUMO+1
E	**16**	**0.1591**	**376.2**	**HOMO−2 → LUMO (37%)**	**HOMO−1 → LUMO+1 (35%)**
F	14	0.0197	387.9	HOMO−3 → LUMO (61%)	HOMO−2 → LUMO+1 (27%)
G	**23**	**0.4415**	**318.0**		**HOMO−12 → LUMO (39%)**
					HOMO−5 → LUMO (34%)
H	21	0.0307	326.4		HOMO−6 → LUMO (62%)
					HOMO−8 → LUMO (24%)

[a] For the molecular orbital assignment, only molecular orbital contributions >10% are listed. [b] Figure 17. [c] Sum of individual oscillator strengths f_I. [d] Weighted average using oscillator strengths. [e] Qualitative molecular orbital assignments for absorption band D are representative of the major contributions from the four excited states.

Vertical transition energies and oscillator strengths for the first 24 excited states were calculated using TD-DFT and the simulated electronic absorption spectrum was calculated using the *SWizard program*.[66] The absorption profile has been deconvoluted as the sum of Gaussian-shaped bands using eq 4, where ϵ is the molar absorption coefficient (in mol^{-1}

$$\epsilon(\omega) = 2.174 \times 10^8 \sum_I \frac{f_I}{\Delta_{1/2,I}} \exp\left[-2.773 \frac{(\omega - \omega_I)^2}{\Delta_{1/2,I}^2}\right] \quad (4)$$

$$\sum_I f_I = 4.319 \times 10^{-9} \int \epsilon(\omega)\, d\omega \quad (5)$$

dm^3 cm^{-1}) and ω_I (in cm^{-1}) is the energy of transition I with associated oscillator strength f_I (dimensionless) and half-bandwidth $\Delta_{1/2,I}$ (in cm^{-1}). The total integrated intensity under the absorption profile is equal to the sum of the oscillator strengths (eq 5). For low-resolution spectroscopy, Gaussian functions have been demonstrated to accurately reproduce experimental band shapes.[67] Qualitatively, the best simulated spectrum was calculated using a half-bandwidth, $\Delta_{1/2}$, of 4500 cm^{-1} for each transition.

The calculated gas-phase TD-DFT spectrum (Figure 18) is in excellent quantitative agreement with the experimental UV/vis spectrum of Cu^{II}ATSM in DMF.[49] In total, 11 excited states with nonzero oscillator strengths contribute to the intensity of the simulated spectrum. The overall shape of the spectrum is accurately reproduced, and the relative absorbance of all peaks and shoulders closely match those observed experimentally. The average wavelength of bands A−C (weighted using the calculated oscillator strengths) gives a predicted absorption peak at 506 nm, which is in excellent agreement with the midpoint between the experimentally observed peak at 476 nm and the shoulder at 525 nm. The intense peak at 314 nm and the shoulder at 355 nm in the experimental spectrum occur at 318 nm and approximately 380 nm in the simulated spectrum. Both the shoulder and peak are composed of two major bands (E and G) and two minor bands (F and H), respectively. The only slight discrepancy occurs in the calculated absorption profile between 450 and 600 nm. This spectroscopic feature is a composite of three absorption bands A−C associated with electronic excitation to excited states 5, 7, and 8, respectively.

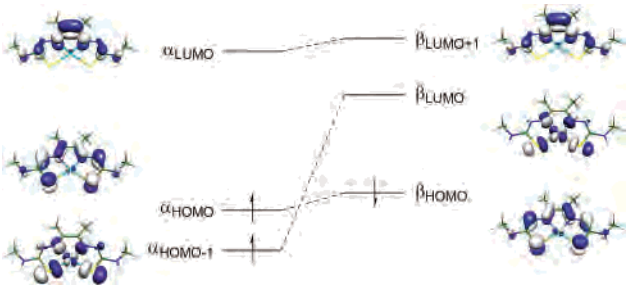

Figure 19. Schematic molecular orbital diagram of Cu^{II}ATSM showing the spatial distribution and relative energy of the frontier orbitals in both the α- and β-spin orbital manifolds. Orbitals with similar spatial distribution are connected by dashed lines.

Deconvolution of each spectroscopic absorption band into associated excited states and the molecular orbital contributions to these transitions are given in Table 5. Spatial distributions of the molecular orbitals involved in the electronic transitions are presented in the Supporting Information. Figure 19 shows a schematic molecular orbital diagram of Cu^{II}ATSM. The unpaired electron is located in the α-spin orbital manifold and is localized in the αHOMO−1 orbital. The αHOMO and αLUMO orbitals have spatial distributions similar to those of the βHOMO and βLUMO+1 orbitals, respectively. The βLUMO orbital is the spatial counterpart of the αHOMO−1 orbital and has in-plane σ*-antibonding character between the copper(II) d_{yz} orbital and the nitrogen and sulfur donor atoms. A detailed

(66) Gorelsky, S. I. *SWizard program*; Department of Chemistry, York University: Toronto, Ontario, Canada, 1998. http://www.sg-chem.net/.
(67) Pearl, G. M.; Zerner, M. C.; Broo, A.; McKelvey, J. *J. Comput. Chem.* **1998**, *19* (7), 781.

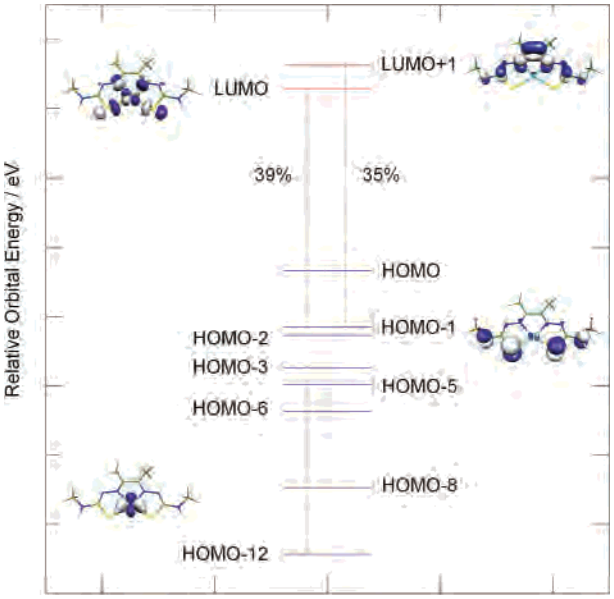

Figure 20. Schematic molecular orbital diagram of the β-spin manifold. Occupied orbitals are shown as blue lines and virtual orbitals as red lines. The vertical black lines represent two of the major molecular orbital transitions involved in the formation of excited state 23 (HOMO−12 → LUMO, 39%) and excited state 16 (HOMO−1 → LUMO+1, 35%). These transitions are associated with spectroscopic absorption bands G and E, respectively. These two bands represent the peak at 314 nm and the associated shoulder at 355 nm in the experimental UV/vis spectrum of CuATSM (Figure 17).

description of the orbitals and bonding in CuATSM has been reported previously.[43]

Figure 20 shows a schematic molecular orbital transition diagram of the β-manifold of Cu^{II}ATSM. Occupied orbitals are shown in blue and virtual orbitals in red. The two vertical black lines represent the most important molecular orbital contributions to the change in the electron density associated with absorption bands E and G. Band G is the major component of the most intense peak in the experimental spectrum at 314 nm and represents an electronic transition from the ground state to excited state 23. The change in the electron density that occurs on forming excited state 23 can be described in terms of the redistribution of the electron density between ground-state molecular orbitals. In this case, two major molecular orbital contributions are involved in the electron density redistribution, which from Table 5 are transitions of βHOMO−12 → βLUMO and of βHOMO−5 → βLUMO. These transitions occur in the β-spin orbital manifold and represent 39% and 34% of the total movement of the electron density on forming excited state 23, respectively. From the spatial distribution of the orbitals shown on the left-hand side in Figure 20, it can be seen that the βHOMO−12 → βLUMO transition involves a movement of the electron density from the copper(II) ion to the in-plane metal−ligand σ* orbital. Therefore, the major absorption band at 314 nm is assigned as a metal-to-ligand charge transfer, which accounts for the relatively large molar absorption coefficient (ϵ > 24 000 mol^{-1} dm^{-3} cm^{-1}).

The major β-spin orbital contribution to the change in the electron density associated with absorption band E is shown on the right-hand side in Figure 20. This band corresponds to the shoulder at 355 nm in the experimental spectrum and involves an electronic transition from the ground state to excited state 16. Significant redistribution of the electron density occurs within both the α- and β-spin orbital manifolds, and the major transitions are of αHOMO−2 → αLUMO and βHOMO−1 → βLUMO+1. These orbital transitions represent 37% and 35% of the total redistribution of the electron density on forming excited state 16. The β-spin orbital component involves a movement of the electron density from the lone pairs of electrons on the sulfur atoms to the vacant π orbital of the carbon−carbon backbone and the donor nitrogen atoms. Similar analysis may be performed for each excited-state transition.

TD-DFT analysis helps us understand the difference in color observed between the yellow zinc(II) and red/brown copper(II) complexes of bis(thiosemicarbazonato) ligands. The d^9 copper(II) complexes possess a hole in the β-spin orbital manifold (βLUMO) corresponding to the metal−ligand σ*-antibonding orbital. Each of the calculated low-energy absorption bands, A−D, involves major molecular orbital transitions from occupied β-orbitals to the vacant βLUMO. In the d^{10} zinc(II) complexes, this orbital is occupied, which means that, upon excitation, only higher energy ligand-based orbitals can be used to accept the redistribution of the electron density. The presence of the low-lying hole in the β-spin orbitals accounts for the red-shift of approximately 50 nm observed in the first spectroscopic band in the experimental UV/vis spectra of zinc(II) and copper(II) bis(thiosemicarbazonato) complexes (Figure 12 and Table 3).

Confocal Fluorescence Microscopy. The intrinsic fluorescence of zinc(II) bis(thiosemicarbazonato) complexes has been used previously to measure cellular uptake and intracellular localization in a range of different cancer cell phenotypes.[31] In this work, confocal fluorescence microscopy experiments were performed using IGROV human ovarian cancer cells under normoxic conditions. Cells were grown in 3.0 mL of a DMEM medium in Petri dishes equipped with an aperture covered by a circular microscope slide coated with polylysine to ensure cell adhesion. Each Petri dish contained around 12 000 cells. After 24 h of incubation at 38.0 °C, background fluorescence images were recorded before the addition of solutions of either ZnATSM/A (**12**) or ZnATSE/A-Glc (**21**) to the extracellular medium. Final concentrations of the zinc(II) complex were approximately 30 μmol dm^{-3}. The mechanism of intracellular trapping is thought to involve a potential protonation step.[43] Therefore, after the fluorescence of the zinc(II) complexes was recorded, the same sample of cells was labeled with LysoTracker, a staining agent that localizes in all acidic organelles, such as lysosomes and endocytotic vesicles. The final concentration of LysoTracker was between 50 and 75 nmol dm^{-3}, and images were recorded after 10−20 min of incubation. Control experiments involving the addition of zinc chloride showed no fluorescence above the very low-intensity background. Previous experiments have also shown that free bis(thiosemicarbazone) proligands are not fluorescent. This demonstrates

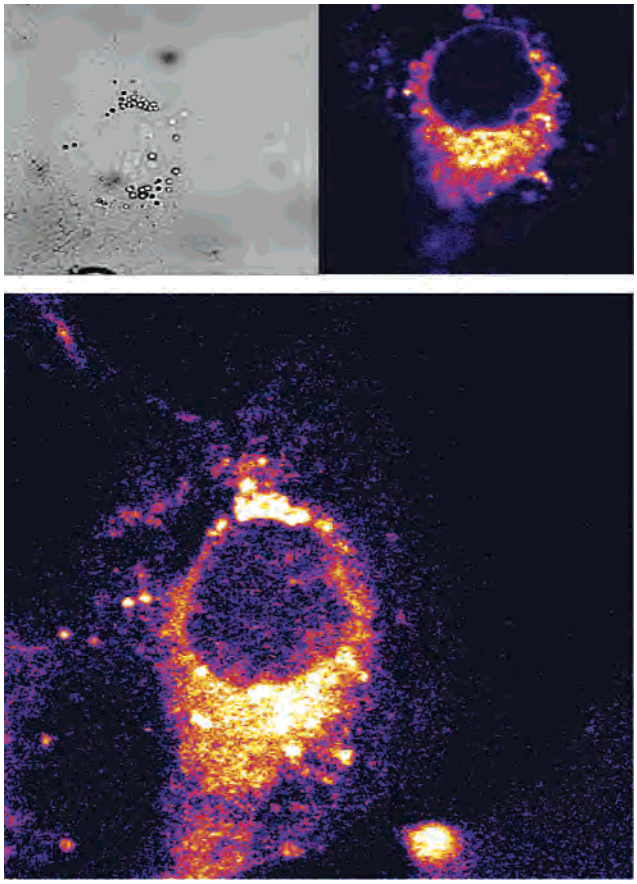

Figure 21. Confocal fluorescence microscopy images of an IGROV human ovarian cancer cell: (top left) bright-field image; (top right) close-up view of LysoTracker fluorescence (λ_{ex} = 568 nm; λ_{em} = 605 nm); (bottom) fluorescence of the zinc(II) complex **12** (λ_{ex} = 488 nm; λ_{em} = 530 nm). The nucleus is visible as the spherical region within the cell showing very little fluorescence.

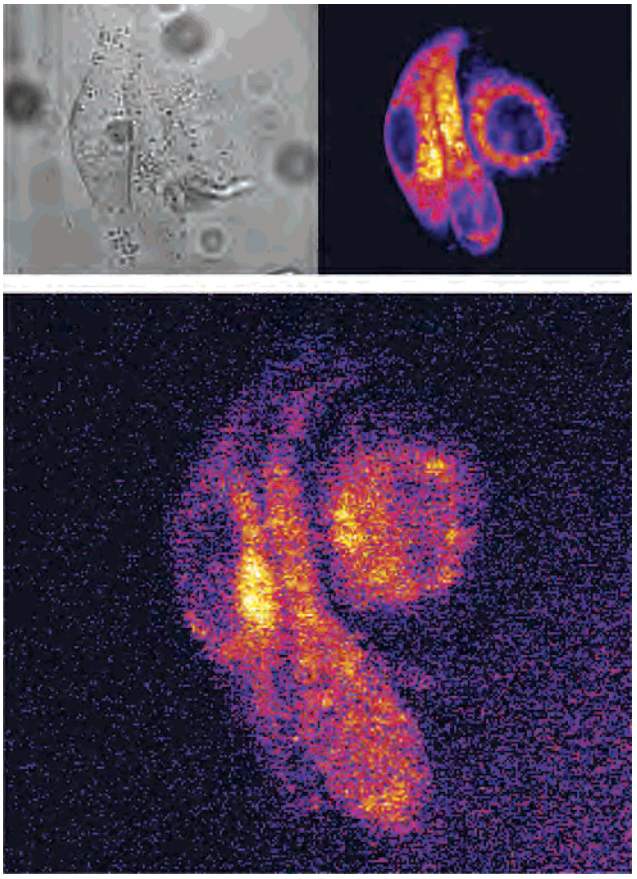

Figure 22. Confocal fluorescence microscopy images of three IGROV human ovarian cancer cells: (top left) bright-field image; (top right) LysoTracker fluorescence (λ_{ex} = 568 nm; λ_{em} = 605 nm); (bottom) fluorescence of the zinc(II) complex **21** (λ_{ex} = 365 nm; λ_{em} = 530 nm). The nucleus is visible in the LysoTracker image as the spherical region within the cells showing very little fluorescence.

that the observed fluorescence is due to the presence of the intact zinc(II) bis(thiosemicarbazonato) chromophore.[31]

Figures 21 and 22 show the fluorescence images recorded with ZnATSM/A (**12**) and ZnATSE/A-Glc (**21**), respectively, after 25−45 min of incubation. Initial, gray-scale fluorescence images were processed using *ImageJ*.[68] In each case, the fluorescence images shown are representative of the response observed across the entire population. Bright-field images were recorded immediately prior to irradiation and fluorescence measurements. Cell uptake was slower for the lipophilic complex (**12**) than the water-soluble glucose conjugate (**21**), with initial intracellular fluorescence being observed in 25−30 and 5−10 min, respectively. The contrast between background fluorescence in solution and fluorescence from within the cells is lower for the zinc(II) complexes than in the images with LysoTracker. This is due to the relatively weak fluorescence emission of the zinc(II) bis(thiosemicarbazonato) fluorophores.

The results demonstrate that both the lipophilic complex, **12**, and the hydrophilic glucose species, **21**, traverse the cell membrane and accumulate in IGROV cells. The mechanism of cellular uptake is unclear and could potentially involve either facilitated diffusion or active transport through intrinsic membrane proteins. The fluorescence images for complex **12** show potential intracellular localization but also show a more diffuse, weaker fluorescence within the cytosol. The fluorescence images of complex **21** are of insufficient resolution to identify any intracellular localization. However, they do demonstrate that the glucose species **21** rapidly enters and accumulates within cells. In both cases, comparison with the LysoTracker images shows similar intracellular distribution, which lends support to the hypothesis of a trapping mechanism involving protonation.[43] Uptake in the nucleus was not observed for either complex **12** or **21** in IGROV cells. Further investigations using additional staining agents are required to identify specific intracellular organelles and to elucidate the mechanism of cellular uptake and trapping of zinc(II) bis(thiosemicarbazonato) complexes. Uptake of these species and other related complexes in breast, prostate, bladder, and skin cancer cells is under investigation to study the cell line dependence and identify structure−activity relationships.

Summary and Conclusions

Two new types of unsymmetrical bis(thiosemicarbazonato) complexes with pendent amino and allyl groups have been synthesized via the isolation of monoketobis(thiosemicar-

(68) Rasband, W. S. *ImageJ*; U.S. National Institutes of Health: Bethesda, MD, 1997−2006. http://rsb.info.nih.gov/ij/.

bazone) intermediates. The zinc(II) complexes of each bis(thiosemicarbazone) proligand, **6**−**11**, have been synthesized and fully characterized using a range of spectroscopic and chromatographic techniques, including EPR, UV/vis, fluorescence, and reverse-phase HPLC. These complexes are the first to be reported that provide a reactive amino group, which can be used to couple BAMs to the bis(thiosemicarbazonato) core. Four crystal structures, including two different zinc(II) complexes are presented. Three novel water-soluble glucose species, **20**−**22**, have been synthesized from zinc(II) complexes with pendent amino groups and have been characterized by HPLC, mass spectrometry, NMR, and other spectroscopic techniques. Copper(II) analogues, **23**−**25**, have been prepared via transmetalation in water using copper(II) acetate. In addition, two copper(II) complexes, **18** and **19**, have been isolated and characterized. Results from electrochemistry experiments indicate that these two complexes have copper(II/I) one-electron-reduction potentials that lie within the biological window to potentially confer hypoxia selectivity.

Copper-64-radiolabeled complexes of **19** and **24** have been prepared in solution and characterized by radio-HPLC. The preparation of ^{64}CuATSE/A-Glc (**24**) demonstrates that transmetalation may be used as a viable method for radiolabeling. Preliminary cell uptake and washout studies using neutrophil cells indicate that under normoxic conditions uptake of the copper-64-radiolabeled complex **24** is rapid and reversible. Investigations to look at cellular uptake and trapping under hypoxic conditions are underway.

The electronic absorption and fluorescence emission spectra of all zinc(II) complexes, **12**−**22**, have been measured, and confocal fluorescence microscopy studies using IGROV cancer cells has shown that zinc(II) bis(thiosemicarbazonato) complexes **12** and **21** accumulate in cells. Labeling studies using LysoTracker indicate that these complexes potentially localize in acidic intracellular compartments.

DFT calculations have been used to investigate the energetics of transmetalation and the nature of the transitions in the electronic absorption spectrum of copper(II) bis(thiosemicarbazonato) complexes.

Conjugation of the free amino group of complexes **12**−**15** with other BAMs, including amino acids and nitroimidazoles, has already been achieved, and these results will be presented in future publications. Studies into protein labeling, including antibody labeling, are underway, and the reactivity of the pendent allyl group is being investigated. Overall, the complexes presented represent a versatile platform for the rapid functionalization of potentially hypoxia-selective copper(II) bis(thiosemicarbazonato) species.

Experimental Section

General Procedures. All reagents and solvents were obtained from commercial sources (Sigma−Aldrich and Lancaster) and, unless otherwise stated, were used as received. Elemental analyses were performed by the microanalysis service of the department at the University of Oxford. NMR spectra were recorded on either a Varian Mercury VX300 spectrometer (^{1}H NMR at 300 MHz and ^{13}C{^{1}H} NMR at 75.5 MHz) or a Varian Unity 500-MHz spectrometer (^{1}H NMR at 499.9 MHz and ^{13}C{^{1}H} NMR at 125.7 MHz) using the residual solvent signal as an internal reference. Mass spectra were recorded on a Micromass LCT time-of-flight mass spectrometer using positive ion electrospray (ES^+), solid probe electron impact (EI), or field ionization (FI^+) techniques. Where possible, accurate masses are reported to four decimal places using tetraoctylammonium bromide (466.5352 Da) as an internal reference. UV/vis spectra were recorded on a Perkin-Elmer Lambda 19 UV/vis/near-IR spectrometer. Fluorescence emission spectra were recorded on a Hitachi F-4500 fluorescence spectrophotometer. EPR spectra were recorded using a Bruker EMX spectrometer calibrated with diphenylpicrylhydrazyl ($g_{iso} = 2.0035$). HPLC was conducted using a Gilson HPLC machine equipped with a Hamilton PRP-1 reverse-phase column and UV/vis detection at 254 nm. Retention times, R_t/min, using a water/acetonitrile gradient elution method, shown in the Supporting Information, are presented for all compounds. Cyclic voltammograms of approximately 1.0 mmol dm^{-3} solutions of complexes **18** and **19** in 5.0 mL of anhydrous DMF were recorded on a CH Instruments electrochemical analyzer using a platinum working electrode, a platinum wire counterelectrode/auxiliary electrode, and a silver/silver ion reference electrode. Ferrocene was used as an internal reference for which the one-electron redox process occurs at $E_{1/2} = 0.53$ V (DMF) vs SCE.

Syntheses. Diacetylbis(4-*N*-methyl-3-thiosemicarbazonato)copper(II), CuATSM, was synthesized in accordance with a previously reported procedure.[38] MS (ES^+): *m/z* (calcd) 322.0099 (322.0096) {M + H$^+$}. λ_{max}(DMF)/nm 525sh (ϵ/mol^{-1} dm^{-3} cm^{-1} 4117), 476 (7855), 355sh (12 018), and 314 (24 061). HPLC: $R_t = 13.15$ min.

The synthesis of 4-*N*-allyl-3-thiosemicarbazide (**1**) was based on a procedure described by Scovill.[44]

Compound 1. Carbon disulfide (6.2 mL, 7.85 g, 0.103 mol) was added to 100 mL of a 1.05 M solution of sodium hydroxide (4.20 g, 0.105 mol) in deionized water at 0 °C. Allylamine (7.7 mL, 5.86 g, 0.103 mol) was added dropwise, and the mixture was allowed to warm to room temperature with continuous stirring for 4 h. Upon the addition of allylamine, an initial pale-pink solution formed, which became a clear-bright orange color after 4 h. A total of 1 equiv of sodium chloroacetate (12.00 g, 0.103 mol) was then added, and the reaction became clear yellow. After stirring overnight at room temperature, a bright-orange solution formed. Excess hydrazine hydrate (25.0 mL, 25.74 g, 0.803 mol) was added, and the mixture was heated under reflux for 4 h. The pale-pink solution was cooled and left to stand overnight in the fridge. The white precipitate was isolated by filtration, washed with water (3 × 20 mL), and dried in vacuo to give compound **1** as a white microcrystalline solid (7.44 g, 57 mmol, 55%). Mp: 92−94 °C (lit. 93−96 °C). Elem anal. Found (calcd) for $C_4H_9N_3S$: C, 36.5 (36.6); H, 6.9 (6.9); N, 32.0 (32.0); S, 24.5 (24.4). ^{1}H NMR (300 MHz, DMSO-d_6): δ/ppm 8.71 (1H, s, NHC(=S)N*H*N=), 7.89 (1H, br s, CH_2N*H*C(=S)NHN), 5.86 (1H, ddt, $^3J_{HH} = 17.3$, 10.3, and 5.3 Hz, CH_2=C*H*CH_2), 5.11 (1H, pseudo dq, $^3J_{HH} = 17.3$, $^2J_{HH}$ and $^4J_{HH} \approx 1.6$ Hz, *trans*-C*H*$_2$=CHCH$_2$NH), 5.04 (1H, pseudo dq, $^3J_{HH} = 10.3$, $^2J_{HH}$ and $^4J_{HH} \approx 1.6$ Hz, *cis*-C*H*$_2$=CHCH$_2$NH), 4.49 (2H, s, NHN*H*$_2$), 4.11 (2H, m, C*H*$_2$NH). ^{13}C{^{1}H} NMR (75.5 MHz, DMSO-d_6): δ/ppm 181.27 (*C*=S), 135.52 (CH_2=*C*HCH_2), 115.09 (*C*H$_2$=CHCH$_2$), 45.13 (CH$_2$=CH*C*H$_2$). MS (ES^+): *m/z* 132 {M + H$^+$}. HPLC: R_t 5.19 min.

General Procedure A: Synthesis of Diacetyl-2-(4-*N*-substituted 3-thiosemicarbazones). 4-*N*-Substituted 3-thiosemicarbazide was added to 100 mL of deionized water and vigorously stirred at 0 °C. Then 5 drops of concentrated HCl was added followed by the rapid addition of 1.2 equiv of 2,3-butadione from a syringe.

The yellow solution quickly became opaque as a white precipitate formed. After 1 h, the precipitate was collected by filtration, washed thoroughly with water (3 × 30 mL), dried in air on filter paper overnight, and then dried in vacuo to give the corresponding diacetyl-2-(4-*N*-substituted 3-thiosemicarbazone) in good yield (>75%). The compounds may be recrystallized from hot aqueous ethanol.

Diacetyl-2-(4-*N*-methyl-3-thiosemicarbazone) (2). As per general procedure A, 2,3-butadione (3.5 mL, 3.43 g, 39.9 mmol) was added to 4-*N*-methyl-3-thiosemicarbazide (3.45 g, 32.8 mmol). Compound **2** was isolated as a white solid (5.03 g, 29.0 mmol, 89%). Mp: 157−159 °C. Elem anal. Found (calcd) for $C_6H_{11}N_3OS$: C, 41.4 (41.6); H, 6.4 (6.4); N, 24.6 (24.3); S, 18.2 (18.5). ^{1}H NMR (300 MHz, DMSO-d_6): δ/ppm 10.65 (1H, s, C(=S)N*H*N=), 8.62 (1H, br m, MeN*H*C(=S)), 3.05 (3H, d, $^3J_{HH}$ = 4.6 Hz, CH_3NH), 2.42 (3H, s, CH_3C=O), 1.96 (3H, s, CH_3C=N). ^{13}C{^{1}H} NMR (75.5 MHz, DMSO-d_6): δ/ppm 197.45 (*C*=O), 178.90 (*C*=S), 145.45 (*C*=N), 31.37 (*C*H$_3$NH), 24.73 (*C*H$_3$C=O), 9.99 (*C*H$_3$C=N). MS (FI$^+$): *m/z* (calcd) 173.0619 (173.0623) {M$^+$}. HPLC: R_t 8.23 min.

Diacetyl-2-(4-*N*-ethyl-3-thiosemicarbazone) (3). As per general procedure A, 2,3-butadione (1.8 mL, 1.77 g, 20.5 mmol) was added to 4-*N*-ethyl-3-thiosemicarbazide (2.00 g, 16.8 mmol). Compound **3** was isolated as a white powder (2.63 g, 14.0 mmol, 84%). Mp: 127−129 °C. Elem anal. Found (calcd) for $C_7H_{11}N_3OS$: C, 44.6 (44.9); H, 7.2 (7.0); N, 22.7 (22.4); S, 17.2 (17.1). ^{1}H NMR (300 MHz, DMSO-d_6): δ/ppm 10.57 (1H, s, C(=S)N*H*N=), 8.66 (1H, br t, CH$_2$N*H*), 3.63 (2H, m, $^3J_{HH}$ = 7.1 Hz, CH$_3$C*H*$_2$NH), 2.42 (3H, s, C*H*$_3$C=O), 1.96 (3H, s, C*H*$_3$C=N), 1.15 (3H, t, $^3J_{HH}$ = 7.1 Hz, C*H*$_3$CH$_2$). ^{13}C{^{1}H} NMR (75.5 MHz, DMSO-d_6): δ/ppm 197.43 (*C*=O), 177.89 (*C*=S), 145.48 (*C*=N), 38.71 (CH$_3$C*H*$_2$), 24.72 (*C*H$_3$C=O), 14.06 (C*H*$_3$CH$_2$), 9.99 (*C*H$_3$C=N). MS (ES$^+$): *m/z* (calcd) 188.0855 (188.0858) {M + H$^+$}. HPLC: R_t 9.67 min.

Diacetyl-2-(4-*N*-phenyl-3-thiosemicarbazone) (4). As per general procedure A, 2,3-butadione (1.2 mL, 1.18 g, 13.7 mmol) was added to 4-*N*-phenyl-3-thiosemicarbazide (1.71 g, 10.2 mmol). Compound **4** was isolated as a cream/white solid (2.12 g, 9.0 mmol, 88%). Mp: 159−161 °C (dec). Elem anal. Found (calcd) for $C_{11}H_{13}N_3OS$: C, 56.2 (56.2); H, 5.6 (5.6); N, 18.0 (17.9); S, 13.5 (13.6). ^{1}H NMR (300 MHz, DMSO-d_6): δ/ppm 10.98 (1H, s, C(=S)N*H*N=), 10.20 (1H, s, PhN*H*), 7.55 (2H, *o-Ph*), 7.40 (2H, *m-Ph*), 7.25 (1H, *p-Ph*), 2.48 (3H, s, C*H*$_3$C=O), 2.03 (3H, s, C*H*$_3$C=N). ^{13}C{^{1}H} NMR (75.5 MHz, DMSO-d_6): δ/ppm 197.55 (*C*=O), 177.66 (*C*=S), 146.29 (*C*=N), 138.71 (*p-Ph*), 128.19 (*m-Ph*), 125.81 (*o-Ph*), 125.76 (*i-Ph*), 24.90 (*C*H$_3$C=O), 10.29 (*C*H$_3$C=N). MS (solid probe EI$^+$): *m/z* (calcd) 235.0774 (235.0779) {M + H$^+$}. HPLC: R_t 12.15 min.

Diacetyl-2-(4-*N*-allyl-3-thiosemicarbazone) (5). As per general procedure A, 2,3-butadione (1.6 mL, 1.57 g, 18.2 mmol) was added to **1** (2.00 g, 15.2 mmol). Compound **5** was isolated as a fine white powder (2.30 g, 11.6 mmol, 76%). Mp: 95−97 °C. Elem anal. Found (calcd) for $C_8H_{13}N_3OS$: C, 47.9 (48.2); H, 6.4 (6.6); N, 21.3 (21.1); S, 16.1 (16.1). ^{1}H NMR (300 MHz, DMSO-d_6): δ/ppm 10.70 (1H, s, NHC(=S)N*H*N=), 8.80 (1H, br m, CH$_2$N*H*C(=S)-NHN), 5.91 (1H, ddt, $^3J_{HH}$ = 17.3, 10.4, and 5.3 Hz, CH$_2$=C*H*CH$_2$), 5.22−5.08 (2H, m, C*H*$_2$=CHCH$_2$), 4.25 (2H, m, CH$_2$=CHC*H*$_2$-NH), 2.42 (3H, s, C*H*$_3$C=O), 1.97 (3H, s, C*H*$_3$C=N). ^{13}C{^{1}H} NMR (75.5 MHz, DMSO-d_6): δ/ppm 197.42 (*C*=O), 178.53 (*C*=S), 145.73 (*C*=N), 134.36 (CH$_2$=*C*HCH$_2$), 115.64 (*C*H$_2$=CHCH$_2$), 46.04 (CH$_2$=CH*C*H$_2$), 24.73 (*C*H$_3$C=O), 10.06 (*C*H$_3$C=N). MS (ES$^+$): *m/z* (calcd) 200.0851 (200.0858) {M + H$^+$}. HPLC: R_t 10.30 min. Crystals suitable for single-crystal X-ray diffraction were grown by vapor diffusion using a DMSO/water solvent system.

General Procedure B: Synthesis of Diacetyl-2-(4-*N*-R$_3$-3-thiosemicarbazone)-3-(4-*N*-R$_4$-3-thiosemicarbazone), Unsymmetrical Bis(thiosemicarbazone) Proligands, H$_2$ATSR$_3$/R$_4$. Thiocarbohydrazide was added to 80 mL of ethanol and the suspension stirred at 50 °C. A total of 1 equiv of 4-N-substituted monoketothiosemicarbazone was added in portions over 2 h. After the final addition, 5 drops of 10% HCl(aq) was added and the reaction heated under reflux for 5 h, during which time a cream/white suspension formed. The mixture was allowed to cool to room temperature, and then the precipitate was collected by filtration, washed with ethanol (2 × 30 mL) and copious amounts of diethyl ether (5 × 30 mL), and then dried in vacuo to give the corresponding unsymmetrical bis(thiosemicarbazone) proligand H_2ATSR_3/R_4 in good yield. Compounds **6**−**9** are very sparingly soluble in most common solvents but may be recrystallized from warm DMSO/water. A different procedure was used for the synthesis of compounds **10** and **11** (vide infra).

Diacetyl-2-(4-*N*-methyl-3-thiosemicarbazone)-3-(4-*N*-amino-3-thiosemicarbazone), H$_2$ATSM/A (6). As per general procedure B, **2** (2.40 g, 13.9 mmol) was added over 2 h in portions to thiocarbohydrazide (1.50 g, 14.1 mmol). Compound **6** was isolated as a cream/white powder (3.37 g, 12.9 mmol, 93%). Mp: >210 °C (dec). Elem anal. Found (calcd) for $C_7H_{15}N_7S_2$: C, 32.1 (32.2); H, 6.0 (5.8); N, 37.2 (37.5); S, 24.6 (24.5). ^{1}H NMR (300 MHz, DMSO-d_6): δ/ppm 10.23 (2H, s, NHC(=S)N*H*N=), 9.70 (1H, br s, N*H*NH$_2$), 8.36 (1H, br m, CH$_3$N*H*C(=S)), 4.96 (2H, s, NHN*H*$_2$), 3.01 (3H, d, $^3J_{HH}$ = 4.5 Hz, C*H*$_3$NH), 2.19 (3H, s, C*H*$_3$C=N), 2.18 (3H, s, C*H*$_3$C=N). ^{13}C{^{1}H} NMR (75.5 MHz, DMSO-d_6): δ/ppm 178.35 (CH$_3$NH*C*=S), 175.84 (NH$_2$NH*C*=S), 148.44 (*C*=N), 148.05 (*C*=N), 31.16 (*C*H$_3$NH), 11.61 (*C*H$_3$C=N), 11.56 (*C*H$_3$C=N). MS (solid probe EI$^+$): *m/z* (calcd) 261.0821 (261.0830) {M + H$^+$}. HPLC: R_t 7.65 min.

Diacetyl-2-(4-*N*-ethyl-3-thiosemicarbazone)-3-(4-*N*-amino-3-thiosemicarbazone), H$_2$ATSE/A (7). As per general procedure B, **3** (1.40 g, 7.5 mmol) was added over 2 h in portions to thiocarbohydrazide (0.80 g, 7.5 mmol). Compound **7** was isolated as a white powder (1.83 g, 6.6 mmol, 89%). Mp: >195 °C (dec). Elem anal. Found (calcd) for $C_8H_{17}N_7S_2$: C, 34.9 (34.9); H, 6.3 (6.2); N, 35.7 (35.6); S, 23.2 (23.3). ^{1}H NMR (300 MHz, DMSO-d_6): δ/ppm 10.21 (1H, s, NHC(=S)N*H*N=), 10.14 (1H, s, NHC-(=S)N*H*N=), 9.70 (1H, br s, N*H*NH$_2$), 8.40 (1H, t, $^3J_{HH}$ = 5.9 Hz, CH$_3$CH$_2$N*H*), 4.96 (2H, s, NHN*H*$_2$), 3.59 (2H, m, CH$_3$C*H*$_2$-NH), 2.18 (6H, two overlapping singlets, C*H*$_3$C=N), 1.13 (3H, t, $^3J_{HH}$ = 7.1 Hz, C*H*$_3$CH$_2$NH). ^{13}C{^{1}H} NMR (75.5 MHz, DMSO-d_6): δ/ppm 177.32 (EtNH*C*=S), 175.84 (NH$_2$NH*C*=S), 148.09 (*C*=N), 148.40 (*C*=N), 38.52 (CH$_3$CH$_2$NH), 14.36 (*C*H$_3$CH$_2$NH), 11.63 (*C*H$_3$C=N), 11.57 (*C*H$_3$C=N). MS (ES$^+$): *m/z* (calcd) 276.1071 (276.1065) {M + H$^+$}. HPLC: R_t 8.64 min.

Diacetyl-2-(4-*N*-phenyl-3-thiosemicarbazone)-3-(4-*N*-amino-3-thiosemicarbazone), H$_2$ATSP/A (8). As per general procedure B, **4** (1.20 g, 5.1 mmol) was added over 2 h in portions to thiocarbohydrazide (0.55 g, 5.2 mmol). Compound **8** was isolated as a creamy yellow powder (1.29 g, 4.0 mmol, 78%). Mp: >230 °C (dec). Elem anal. Found (calcd) for $C_{12}H_{17}N_7S_2$: C, 44.4 (44.6); H, 5.3 (5.3); N, 30.1 (30.3); S, 19.5 (19.8). ^{1}H NMR (300 MHz, DMSO-d_6): δ/ppm 10.59 (1H, s, PhN*H* probable tautomerization), 10.29 (1H, s, NHC(=S)N*H*N=), 9.95 (1H, s, NHC(=S)N*H*N=), 9.75 (1H, br s, N*H*NH$_2$), 7.56 (2H, *o-Ph*), 7.37 (2H, *m-Ph*), 7.21 (1H, *p-Ph*), 5.00 (2H, br s, NHN*H*$_2$), 2.27 (3H, s, C*H*$_3$C=N), 2.23 (3H, s, C*H*$_3$C=N). MS (ES$^+$): *m/z* 324 {M + H$^+$}. HPLC: R_t 10.71 min.

Diacetyl-2-(4-*N*-allyl-3-thiosemicarbazone)-3-(4-*N*-amino-3-thiosemicarbazone), H$_2$ATSAllyl/A (9). As per general procedure

B, **5** (1.00 g, 5.0 mmol) was added over 2 h in portions to thiocarbohydrazide (0.53 g, 5.0 mmol). Compound **9** was isolated as a lemon-yellow powder (1.21 g, 4.2 mmol, 84%). Elem anal. Found (calcd) for $C_9H_{17}N_7S_2$: C, 37.3 (37.6); H, 6.0 (6.0); N, 34.0 (34.1); S, 22.2 (22.3). ^{1}H NMR (300 MHz, DMSO-d_6): δ/ppm 10.29 (1H, s, NHC(=S)N*H*N=), 10.22 (1H, s, NHC(=S)N*H*N=), 9.71 (1H, s, N*H*NH$_2$), 8.52 (1H, t, $^3J_{HH}$ = 5.8 Hz, CH$_2$N*H*C(=S)), 5.90 (1H, ddt, $^3J_{HH}$ = 17.3, 10.4, and 5.3 Hz, CH$_2$=C*H*CH$_2$), 5.18−5.06 (2H, m, C*H*$_2$=CHCH$_2$), 4.97 (2H, s, NHN*H*$_2$), 4.22 (2H, m, CH$_2$=CHC*H*$_2$NH), 2.19 (6H, two overlapping singlets, C*H*$_3$C=N). ^{13}C{^{1}H} NMR (75.5 MHz, DMSO-d_6): δ/ppm 177.89 (CH$_2$NH*C*=S), 175.84 (NH$_2$NH*C*=S), 148.40 (*C*=N), 148.34 (*C*=N), 134.78 (CH$_2$=*C*HCH$_2$), 115.46 (*C*H$_2$=CHCH$_2$), 45.89 (CH$_2$=CH*C*H$_2$), 11.63 (2 × *C*H$_3$C=N). MS (ES$^+$): *m/z* (calcd) 310 {M + Na$^+$}. HPLC: R_t 8.72 min.

Diacetyl-2-(4-*N*-methyl-3-thiosemicarbazone)-3-(4-*N*-allyl-3-thiosemicarbazone), H$_2$ATSM/Allyl (10). 5 (1.00 g, 5.0 mmol) was added to a stirred suspension of 4-*N*-methyl-3-thiosemicarbazide (0.53 g, 5.0 mmol) in 75 mL of ethanol. After stirring for 30 min, 5 drops of a 10% HCl(aq) acid catalyst was added and the reaction stirred overnight at 45 °C, during which time a white precipitate formed. The mixture was allowed to cool, and solid was collected by filtration, washed with ethanol (2 × 20 mL) and diethyl ether (3 × 20 mL), and then dried in vacuo. Compound **10** was isolated as a white powder (1.27 g, 4.5 mmol, 89%). Elem anal. Found (calcd) for $C_{10}H_{18}N_6S_2$: C, 41.9 (41.9); H, 6.3 (6.3); N, 29.4 (29.3); S, 22.4 (22.4). ^{1}H NMR (300 MHz, DMSO-d_6): δ/ppm 10.27 (2H, s, 2 × NHC(=S)N*H*N=), 8.54 (1H, t, $^3J_{HH}$ = 5.7 Hz, CH$_2$N*H*), 8.39 (1H, m, CH$_3$N*H*), 5.90 (1H, ddt, $^3J_{HH}$ = 17.3, 10.4, and 5.3 Hz, CH$_2$=C*H*CH$_2$), 5.18−5.02 (2H, m, C*H*$_2$=CH−CH$_2$), 4.22 (2H, m, CH$_2$=CHC*H*$_2$NH), 3.02 (3H, d, $^3J_{HH}$ = 4.5 Hz, C*H*$_3$-NH), 2.22 (3H, s, C*H*$_3$C=N), 2.20 (3H, s, C*H*$_3$C=N). ^{13}C{^{1}H} NMR (75.5 MHz, DMSO-d_6): δ/ppm 178.36 (*C*=S), 177.89 (*C*=S), 148.26 (*C*=N), 147.82 (*C*=N), 134.77 (CH$_2$=*C*HCH$_2$), 115.46 (*C*H$_2$=CHCH$_2$), 45.89 (CH$_2$=CH*C*H$_2$), 31.16 (*C*H$_3$NH), 11.71 (*C*H$_3$C=N), 11.65 (*C*H$_3$C=N). MS (ES$^+$): *m/z* 287 {M + H$^+$}. HPLC: R_t 11.12 min.

Diacetyl-2-(4-*N*-ethyl-3-thiosemicarbazone)-3-(4-*N*-allyl-3-thiosemicarbazone), H$_2$ATSE/Allyl (11). 5 (1.5 g, 7.5 mmol) was added to a stirred suspension of 4-*N*-ethyl-3-thiosemicarbazide (0.9 g, 7.5 mmol) in 75 mL of ethanol. After stirring for 30 min, 5 drops of a 10% HCl(aq) acid catalyst was added and the reaction stirred overnight at 45 °C, during which time a white precipitate formed. The mixture was allowed to cool, and solid was collected by filtration, washed with ethanol (2 × 20 mL) and diethyl ether (3 × 20 mL), and then dried in vacuo. Compound **11** was isolated as a white powder (2.12 g, 7.1 mmol, 95%). Elem anal. Found (calcd) for $C_{11}H_{20}N_6S_2$: C, 43.7 (44.0); H, 6.7 (6.7); N, 27.8 (28.0); S, 21.6 (21.3). ^{1}H NMR (300 MHz, DMSO-d_6): δ/ppm 10.28 and 10.18 (2H, two overlapping singlets, 2 × NHC(=S)N*H*N=), 8.54 (1H, t, $^3J_{HH}$ = 5.8 Hz, CH$_2$=CHCH$_2$N*H*), 8.43 (1H, t, $^3J_{HH}$ = 5.8 Hz, CH$_3$CH$_2$N*H*), 5.90 (1H, ddt, $^3J_{HH}$ = 17.2, 10.3, and 5.3 Hz, CH$_2$=C*H*CH$_2$), 5.19−5.05 (2H, m, C*H*$_2$=CHCH$_2$), 4.22 (2H, m, CH$_2$=CHC*H*$_2$NH), 3.59 (2H, m, CH$_3$C*H*$_2$NH), 3.02 (3H, d, $^3J_{HH}$ = 4.5 Hz, C*H*$_3$NH), 2.22 and 2.20 (6H, two overlapping singlets, C*H*$_3$C=N), 1.13 (3H, t, $^3J_{HH}$ = 7.1 Hz, C*H*$_3$CH$_2$). ^{13}C{^{1}H} NMR (75.5 MHz, DMSO-d_6): δ/ppm 177.88 (*C*=S), 177.31 (*C*=S), 148.19 (*C*=N), 147.82 (*C*=N), 134.76 (CH$_2$=*C*HCH$_2$), 115.47 (*C*H$_2$=CHCH$_2$), 45.90 (CH$_2$=CH*C*H$_2$), 38.51 (CH$_3$*C*H$_2$NH), 14.33 (*C*H$_3$CH$_2$NH), 11.72 (*C*H$_3$C=N), 11.65 (*C*H$_3$C=N). MS (ES$^+$): *m/z* (calcd) 323.1077 (323.1089) {M + H$^+$}. HPLC: R_t 12.24 min. Colorless crystals suitable for single X-ray crystallography were isolated from the NMR sample in DMSO-d_6.

General Procedure C: Synthesis of Unsymmetrical Diacetyl-2-(4-*N*-R$_3$-3-thiosemicarbazonato)-3-(4-*N*-R$_4$-3-thiosemicarbazonato)zinc(II) Complexes, ZnATSR$_3$/R$_4$. Zinc(II) diacetate dihydrate (1.2 equiv) was added to a stirred suspension of a H$_2$ATSR$_3$/R$_4$, unsymmetrical bis(thiosemicarbazone) proligand in 30 mL of methanol. Upon the addition of Zn(OAc)$_2$·2H$_2$O, the reaction turned yellow immediately. The mixture was then heated under reflux for 4 h. A yellow/orange precipitate formed, which, after cooling, was collected by filtration, washed with methanol (2 × 20 mL) and copious amounts of diethyl ether (5 × 30 mL), and then dried in vacuo at 80 °C to give the corresponding ZnATSR$_3$/R$_4$ neutral zinc(II) complexes in excellent yield. Complexes **16** and **17** are soluble in both methanol and diethyl ether. Therefore, the reaction solvent was removed under reduced pressure to <5 mL and cooled at 0 °C overnight. The yellow precipitate was collected by filtration, washed with water (2 × 30 mL), and dried in vacuo to give complexes **16** and **17**. The neutral zinc(II) complexes may be recrystallized from hot methanol.

Diacetyl-2-(4-*N*-methyl-3-thiosemicarbazonato)-3-(4-*N*-amino-3-thiosemicarbazonato)zinc(II) Monomethanol, ZnATSM/A·MeOH (12). As per general procedure C, Zn(OAc)$_2$·2H$_2$O (1.43 g, 6.5 mmol) was added to compound **6** (1.40 g, 5.4 mmol) in 30 mL of methanol. The product was found to contain 1 equiv of methanol, which persisted after 3 days of drying in vacuo at 80 °C. Complex **12** was isolated as a yellow powder (1.87 g, 5.2 mmol, 97%). Mp: >230 °C (dec). Elem anal. Found (calcd) for $C_8H_{17}N_7OS_2Zn$ (methanol included): C, 26.9 (26.9); H, 4.7 (4.8); N, 27.7 (27.5); S, 18.5 (18.0); Zn, 17.9 (18.3). ^{1}H NMR (300 MHz, DMSO-d_6): δ/ppm 8.26 (1H, s, N*H*NH$_2$), 7.25 (1H, br s, CH$_3$N*H*), 4.50 (2H, s, NHN*H*$_2$), 4.11 (1H, q, $^3J_{HH}$ = 5.3 Hz, CH$_3$O*H*), 3.16 (3H, d, $^3J_{HH}$ = 5.3 Hz, C*H*$_3$OH), 2.82 (3H, d, $^3J_{HH}$ = 4.3 Hz, C*H*$_3$NH), 2.23 (3H, s, C*H*$_3$C=N), 2.21 (3H, s, C*H*$_3$C=N). ^{13}C{^{1}H} NMR (75.5 MHz, DMSO-d_6): δ/ppm 178.31 (CH$_3$NH*C*=S), 175.74 (NH$_2$-NH*C*=S), 145.86 (*C*=N), 145.19 (*C*=N), 48.60 (*C*H$_3$OH), 29.21 (*C*H$_3$NH), 14.61 (*C*H$_3$C=N), 13.87 (*C*H$_3$C=N). MS (ES$^+$): *m/z* (calcd) 324.0059 (324.0044) {M + H$^+$}. λ_{max}(DMSO)/nm 431 (ϵ/mol^{-1} dm^{-3} cm^{-1} 11 700) and 314 (10 825). HPLC: R_t 6.87 min. Crystals suitable for single-crystal X-ray diffraction were grown by vapor diffusion using a DMSO/water solvent system.

Diacetyl-2-(4-*N*-ethyl-3-thiosemicarbazonato)-3-(4-*N*-amino-3-thiosemicarbazonato)zinc(II), ZnATSE/A (13). As per general procedure C, Zn(OAc)$_2$·2H$_2$O (1.43 g, 6.5 mmol) was added to compound **7** (1.50 g, 5.4 mmol) in 30 mL of methanol. Complex **13** was isolated as a light-yellow powder (1.75 g, 5.2 mmol, 95%). Mp: >230 °C (dec). Elem anal. Found (calcd) for $C_8H_{15}N_7S_2Zn$: C, 28.4 (28.4); H, 4.6 (4.5); N, 28.6 (28.9); S, 19.1 (18.9); Zn, 18.9 (19.3). ^{1}H NMR (300 MHz, DMSO-d_6): δ/ppm 8.22 (1H, s, N*H*NH$_2$), 7.29 (1H, br s, CH$_3$CH$_2$N*H*), 4.57 (2H, s, NHN*H*$_2$), 3.36 (2H, m obscured by residual HDO, assigned from COSY, CH$_3$C*H*$_2$-NH), 2.22 (3H, s, C*H*$_3$C=N), 2.19 (3H, s, C*H*$_3$C=N), 1.10 (3H, t, $^3J_{HH}$ = 7.2 Hz, C*H*$_3$CH$_2$NH). MS (ES$^+$): *m/z* (calcd) 338.0190 (338.0200) {M + H$^+$}. λ_{max}(DMSO)/nm 433 (ϵ/mol^{-1} dm^{-3} cm^{-1} 12 337). HPLC: R_t 8.10 min.

Diacetyl-2-(4-*N*-phenyl-3-thiosemicarbazonato)-3-(4-*N*-amino-3-thiosemicarbazonato)zinc(II), ZnATSP/A (14). As per general procedure C, Zn(OAc)$_2$·2H$_2$O (0.82 g, 3.7 mmol) was added to compound **8** (1.00 g, 3.1 mmol) in 30 mL of methanol. Complex **14** was isolated as a dark-orange powder (1.06 g, 2.8 mmol, 89%). Mp: >230 °C (dec). Elem anal. Found (calcd) for $C_{12}H_{15}N_7S_2Zn$: C, 37.2 (37.3); H, 3.9 (3.9); N, 25.6 (25.4); S, 17.2 (16.8); Zn, 16.7 (16.9). ^{1}H NMR (300 MHz, DMSO-d_6): δ/ppm 9.37 (1H, s, PhN*H*), 8.50 (1H, br s, N*H*NH$_2$), 7.81 (2H, *o-Ph*), 7.24 (2H, *m-Ph*), 6.91 (1H, *p-Ph*), 2.31 (3H, s, C*H*$_3$C=N), 2.27 (3H, s, C*H*$_3$C=N).

MS (ES^+): *m/z* (calcd) 386.0213 (386.0200) {M + H^+}. λ_{max}(DMSO)/nm 439 (ϵ/mol^{-1} dm^{-3} cm^{-1} 13 919) and 326 (11 981). HPLC: R_t 10.27 min.

Diacetyl-2-(4-*N*-allyl-3-thiosemicarbazonato)-3-(4-*N*-amino-3-thiosemicarbazonato)zinc(II), ZnATSAllyl/A (15). As per general procedure C, $Zn(OAc)_2{\cdot}2H_2O$ (0.27 g, 1.3 mmol) was added to compound **9** (0.3 g, 1.0 mmol) in 30 mL of methanol. Complex **15** was isolated as a bright-yellow powder (0.30 g, 0.9 mmol, 83%). Mp: >230 °C (dec). Elem anal. Found (calcd) for $C_9H_{15}N_7S_2Zn$: C, 30.5 (30.8); H, 4.5 (4.3); N, 27.8 (28.0); S, 18.5 (18.3); Zn, 18.5 (18.6). ^{1}H NMR (300 MHz, DMSO-d_6): δ/ppm 8.27 (1H, s, N*H*NH_2), 7.44 (1H, br s, CH_2N*H*), 5.88 (1H, m, CH_2=C*H*CH_2), 5.18−5.00 (2H, m, C*H*$_2$=CH−CH_2), 4.48 (2H, s, NHN*H*$_2$), 3.96 (2H, m, CH_2=CHC*H*$_2$NH), 2.22 (3H, s, C*H*$_3$C=N), 2.19 (3H, s, C*H*$_3$C=N). MS (ES^+): *m/z* (calcd) 350.0188 (350.0200) {M + H^+}. λ_{max}(DMSO)/nm 433 (ϵ/mol^{-1} dm^{-3} cm^{-1} 11 416) and 314 (10 424). HPLC: R_t 8.17 min.

Diacetyl-2-(4-*N*-methyl-3-thiosemicarbazonato)-3-(4-*N*-allyl-3-thiosemicarbazonato)zinc(II), ZnATSM/Allyl (16). As per general procedure C, $Zn(OAc)_2{\cdot}2H_2O$ (0.27 g, 1.3 mmol) was added to compound **10** (0.3 g, 1.0 mmol) in 30 mL of methanol. Complex **16** was isolated as a bright-yellow powder (0.34 g, 0.97 mmol, 93%). Mp: >230 °C (dec). Elem anal. Found (calcd) for $C_{10}H_{16}N_6S_2Zn$: C, 34.0 (34.3); H, 4.7 (4.6); N, 24.0 (24.0); S, 18.3 (18.3); Zn, 18.4 (18.7). ^{1}H NMR (300 MHz, DMSO-d_6): δ/ppm 7.41 (1H, br s, CH_2N*H*), 7.22 (1H, br s, CH_3N*H*), 5.88 (1H, m, CH_2=C*H*CH_2), 5.18−4.99 (2H, m, C*H*$_2$=$CHCH_2$), 3.96 (2H, m, CH_2=CHC*H*$_2$NH), 2.82 (3H, d, C*H*$_3$$NH_2$), 2.19 (3H, s, C*H*$_3$C=N), 2.18 (3H, s, C*H*$_3$C=N). MS ($ES^+$): *m/z* (calcd) 349.0256 (349.0248) {M + H^+}. λ_{max}(DMSO)/nm 435 (ϵ/mol^{-1} dm^{-3} cm^{-1} 13 264) and 315 (13 512). HPLC: R_t 9.58 min.

Diacetyl-2-(4-*N*-ethyl-3-thiosemicarbazonato)-3-(4-*N*-allyl-3-thiosemicarbazonato)zinc(II), ZnATSE/Allyl (17). As per general procedure C, $Zn(OAc)_2{\cdot}2H_2O$ (0.57 g, 2.6 mmol) was added to compound **11** (0.65 g, 2.2 mmol) in 30 mL of methanol. Complex **17** was isolated as a bright-yellow powder (0.76 g, 2.1 mmol, 96%). Mp: >230 °C (dec). Elem anal. Found (calcd) for $C_{11}H_{18}N_6S_2Zn$: C, 36.2 (36.3); H, 5.0 (5.0); N, 23.1 (23.1); S, 17.6 (17.6); Zn, 18.0 (18.0). ^{1}H NMR (300 MHz, DMSO-d_6): δ/ppm 7.40 (1H, br s, CH_2=$CHCH_2$N*H*), 7.26 (1H, br s, CH_3CH_2N*H*), 5.88 (1H, m, CH_2=C*H*CH_2), 5.18−4.99 (2H, m, C*H*$_2$=$CHCH_2$), 3.95 (2H, m, CH_2=CHC*H*$_2$NH), 3.33 (2H, m obscured by residual water assigned from COSY, CH_3C*H*$_2$NH), 2.18 (6H, s, 2 × C*H*$_3$C=N), 1.10 (3H, t, $^3J_{HH}$ = 7.1 Hz, CH_3C*H*$_2$NH). ^{13}C{^{1}H} NMR (75.5 MHz, DMSO-d_6): δ/ppm 175.18 (CH_3NHC=S), 145.38 (*C*=N) (NB: only two weak quaternary resonances were observed), 135.75 (CH_2=*C*HCH_2), 115.12 (*C*H_2=$CHCH_2$), 44.61 (CH_2=CH*C*H_2), 36.88 (CH_3CH_2), 14.62 (*C*H_3CH_2), 13.87 and 13.79 (2 × *C*H_3C=N). MS (ES^+): *m/z* (calcd) 363.0399 (363.0404) {M + H^+}. λ_{max}(DMSO)/nm 433 (ϵ/mol^{-1} dm^{-3} cm^{-1} 8579) and 314 (8361). HPLC: R_t 10.76 min. Crystals of the methanol adduct, suitable for single-crystal X-ray diffraction, were obtained after leaving the methanolic filtrate at 4 °C for 72 h.

Diacetyl-2-(4-*N*-methyl-3-thiosemicarbazonato)-3-(4-*N*-allyl-3-thiosemicarbazonato)copper(II), CuATSM/Allyl (18). As per general procedure C, $Cu(OAc)_2{\cdot}H_2O$ (0.27 g, 1.3 mmol) was added to compound **10** (0.3 g, 1.0 mmol) in 30 mL of methanol. Complex **18** was isolated as a red/brown powder (0.32 g, 0.9 mmol, 88%). Elem anal. Found (calcd) for $C_{10}H_{16}N_6S_2Cu$: C, 34.8 (34.5); H, 4.7 (4.6); N, 23.9 (24.2); S, 18.8 (18.4); Cu, 17.9 (18.3). MS (ES^+): *m/z* (calcd) 349.0256 (349.0248) {M + H^+}. λ_{max}(DMSO)/nm 476 (ϵ/mol^{-1} dm^{-3} cm^{-1} 5172) and 314 (15 443). HPLC: R_t 14.41 min.

Diacetyl-2-(4-*N*-ethyl-3-thiosemicarbazonato)-3-(4-*N*-allyl-3-thiosemicarbazonato)copper(II), CuATSE/Allyl (19). As per general procedure C, $Cu(OAc)_2{\cdot}H_2O$ (0.48 g, 2.4 mmol) was added to compound **11** (0.6 g, 2.0 mmol) in 30 mL of methanol. Complex **19** was isolated as a red/brown powder (0.68 g, 1.9 mmol, 94%). Elem anal. Found (calcd) for $C_{11}H_{18}N_6S_2Cu$: C, 36.5 (36.5); H, 5.2 (5.0); N, 22.9 (23.2); S, 17.9 (17.7); Cu, 17.3 (17.6). MS (ES^+): *m/z* (calcd) 362.0418 (362.0409) {M + H^+}. λ_{max}(DMSO)/nm 477 (ϵ/mol^{-1} dm^{-3} cm^{-1} 5627) and 315 (16 693). HPLC: R_t 15.57 min. Radio-HPLC (^{64}Cu-**19**): 16.27 min.

General Procedure D: Synthesis of Glucose-Functionalized Zinc(II) Complexes, $ZnATSR_3$/A-Glc. α,β-D-Glucose (1.0 equiv) was added to a stirred suspension of $ZnATSR_3$/A in 30 mL of methanol. A total of 1 drop of 10% HCl(aq) was added as a catalyst. The mixture was then heated under reflux for 12−15 h. During the reaction, the yellow suspension of $ZnATSR_3$/A dissolved, forming a clear red/orange solution. The reaction mixture was concentrated under reduced pressure to <5 mL and cooled to room temperature. The product was precipitated by the dropwise addition of 40 mL of diethyl ether. The yellow solid was collected by filtration, washed with copious amounts of diethyl ether (5 × 20 mL), and then dried in vacuo at 80 °C to give the corresponding $ZnATSR_3$/A-Glc complex.

Diacetyl-2-(4-*N*-methyl-3-thiosemicarbazonato)-3-(4-*N*-amino-(1-β-*N*-glucosyl)-3-thiosemicarbazonato)zinc(II), ZnATSM/A-Glc (20). As per general procedure D, α,β-D-glucose (0.14 g, 0.8 mmol) was added to complex **12** (0.25 g, 0.8 mmol) in 30 mL of methanol with 1 drop of a 10% HCl(aq) catalyst. Complex **20** was isolated as a yellow powder (0.31 g, 0.6 mmol, 84%). ^{1}H NMR (300 MHz, MeOH-d_4): δ/ppm 4.00 (1H, d, $^3J_{1,2}$ = 8.8 Hz, H-1), 3.87 (1H, dd, $^2J_{6a,6b}$ = 11.7 Hz, $^3J_{5,6a}$ = 1.7 Hz, H-6a), 3.68 (1H, dd, $^2J_{6a,6b}$ = 11.7 Hz, $^3J_{5,6b}$ = 4.9 Hz, H-6b), 3.43 (1H, t, $^3J_{2,3}$ = 8.8 Hz, $^3J_{3,4}$ = 8.7 Hz, H-3), approximately 3.30 (1H, m obscured by solvent, H-5), 3.27 (1H, t, $^3J_{3,4}$ = 8.7 Hz, H-4), 3.24 (1H, t, $^3J_{1,2}$ = 8.8 Hz, $^3J_{2,3}$ = 8.8 Hz, H-2), 2.98 (3H, s, C*H*$_3$NH), 2.30 (3H, s, C*H*$_3$C=N), 2.29 (3H, s, C*H*$_3$C=N). ^{13}C{^{1}H} NMR (75.5 MHz, MeOH-d_4): δ/ppm 181.58 (*C*=S), 150.12 (*C*=N) (NB: only two quaternary peaks were observed), 91.61 (C-1), 79.32 (C-5), 77.93 (C-3), 71.62 (C-2), 71.39 (C-4), 62.75 (C-6), 30.03 (CH_3-NH), 14.62 and 14.24 (2 × *C*H_3C=N). MS (ES^+): *m/z* (calcd) 486.0576 (486.0572) {M + H^+}. λ_{max}(H_2O)/nm 403 (ϵ/mol^{-1} dm^{-3} cm^{-1} 8434) and 296 (9899). HPLC: R_t 5.29 min.

Diacetyl-2-(4-*N*-ethyl-3-thiosemicarbazonato)-3-(4-*N*-amino-(1-β-*N*-glucosyl)-3-thiosemicarbazonato)zinc(II), ZnATSE/A-Glc (21). As per general procedure D, α,β-D-glucose (0.13 g, 0.7 mmol) was added to complex **13** (0.25 g, 0.7 mmol) in 30 mL of methanol with 1 drop of a 10% HCl(aq) catalyst. Complex **21** was isolated as a yellow powder (0.34 g, 0.7 mmol, 93%). ^{1}H NMR (300 MHz, MeOH-d_4): δ/ppm 4.02 (1H, d, $^3J_{1,2}$ = 8.8 Hz, H-1), 3.88 (1H, dd, $^2J_{6a,6b}$ = 11.9 Hz, $^3J_{5,6a}$ = 1.6 Hz, H-6a), 3.69 (1H, dd, $^2J_{6a,6b}$ = 11.9 Hz, $^3J_{5,6b}$ = 4.7 Hz, H-6b), 3.50 (2H, t, $^3J_{HH}$ = 7.1 Hz, CH_3C*H*$_2$NH), 3.44 (1H, t, $^3J_{2,3}$ = 8.7 Hz, $^3J_{3,4}$ = 8.7 Hz, H-3), approximately 3.30 (1H, m obscured by solvent, H-5), 3.26 (1H, t obscured, H-4), 3.24 (1H, t, $^3J_{1,2}$ = 8.8 Hz, $^3J_{2,3}$ = 8.8 Hz, H-2), 2.31 (3H, s, C*H*$_3$C=N), 2.29 (3H, s, C*H*$_3$C=N), 1.20 (3H, t, $^3J_{HH}$ = 7.1 Hz, C*H*$_3$$CH_2$NH). ^{13}C{^{1}H} NMR (75.5 MHz, MeOH-d_4): δ/ppm (NB: no quaternary *C*=S peaks were observed and only one *C*=N resonance was observed) 152.04 (*C*=N), 91.51 (C-1), 79.33 (C-5), 78.04 (C-3), 71.74 (C-2), 71.47 (C-4), 62.75 (C-6), 39.00 (CH_3C*H*$_2$NH), 14.99 and 14.20 (2 × *C*H_3C=N). MS (ES^+): *m/z* (calcd) 500.0717 (500.0728) {M + H^+}. λ_{max}(H_2O)/nm 404 (ϵ/mol^{-1} dm^{-3} cm^{-1} 8866) and 296 (9670). HPLC: R_t 5.63 min.

Diacetyl-2-(4-*N*-allyl-3-thiosemicarbazonato)-3-(4-*N*-amino-(1-β-*N*-glucosyl)-3-thiosemicarbazonato)zinc(II), ZnATSAllyl/A-Glc (22). As per general procedure D, α,β-D-glucose (0.13 g, 0.7 mmol) was added to complex **15** (0.25 g, 0.7 mmol) in 30 mL of methanol with 1 drop of a 10% HCl(aq) catalyst. Complex **22** was isolated as a yellow powder (0.32 g, 0.6 mmol, 88%). ^{1}H NMR (500 MHz, MeOH-d_4): δ/ppm 5.93 (1H, ddt, $^3J_{HH}$ = 17.2, 10.3, and 5.6 Hz, CH_2=C*H*CH_2), AB system 5.20 (1H, pseudo dq, $^3J_{HH}$ = 17.2, $^2J_{HH}$ and $^4J_{HH}$ = 1.6 Hz, *trans*-C*H*$_2$=$CHCH_2$NH), 5.08 (1H, pseudo dq, $^3J_{HH}$ = 10.3, $^2J_{HH}$ and $^4J_{HH}$ = 1.3 Hz, *cis*-C*H*$_2$=$CHCH_2$NH), 4.09 (2H, br m, CH_2=CHC*H*$_2$NH), 4.00 (1H, d, $^3J_{1,2}$ = 8.9 Hz, H-1), 3.87 (1H, dd, $^2J_{6a,6b}$ = 11.8 Hz, $^3J_{5,6a}$ = 2.1 Hz, H-6a), 3.68 (1H, dd, $^2J_{6a,6b}$ = 11.7 Hz, $^3J_{5,6b}$ = 5.3 Hz, H-6b), 3.42 (1H, t, $^3J_{2,3}$ = 9.0 Hz, $^3J_{3,4}$ = 8.8 Hz, H-3), approximately 3.30 (1H, m obscured by solvent, H-5), 3.27 (1H, t, $^3J_{3,4}$ = 8.8 Hz, H-4), 3.24 (1H, t, $^3J_{1,2}$ = 8.9 Hz, $^3J_{2,3}$ = 9.0 Hz, H-2), 2.29 (3H, s, C*H*$_3$C=N), 2.27 (3H, s, C*H*$_3$C=N). ^{13}C{^{1}H} NMR (125.7 MHz, MeOH-d_4): δ/ppm 181.29 (*C*=S), 150.09 (*C*=N) (NB: only two weak quaternary resonances were observed), 136.21 (CH_2=*C*HCH_2), 116.10 (*C*H_2=$CHCH_2$), 91.48 (C-1), 79.22 (C-5), 77.90 (C-3), 71.53 (C-2), 71.36 (C-4), 62.68 (C-6), 46.36 (CH_2=CH*C*H_2), 14.63 and 14.24 (2 × *C*H_3C=N). MS (ES$^+$): *m/z* (calcd) 512.0724 (512.0728) {M + H$^+$}. λ_{max}(H_2O)/nm 405 (ϵ/mol^{-1} dm^{-3} cm^{-1} 9531) and 298 (10 801). HPLC: R_t 5.63 min.

Transmetalation. Aqueous solutions of copper(II) complexes of the three glucose-functionalized zinc(II) complexes described above were prepared via transmetalation by the following procedure.

A Zn$ATSR_3$/A-Glc complex, **20**−**22**, was dissolved in water, forming a vivid-yellow solution, and diluted to a concentration of 1.0 mmol dm^{-3}. A stock solution of 0.1 mol dm^{-3} Cu$(OAc)_2$(aq) was prepared separately. The corresponding Cu$ATSR_3$/A-Glc complex was prepared in situ by mixing 3.0 mL aliquots of the Zn$ATSR_3$/A-Glc(aq) solution with 1 equiv of (0.01 mol dm^{-3}) Cu$(OAc)_2$(aq). The reaction was rapid (<1 s), and the mixture changed to a red/brown color as the zinc(II) ions were displaced and the copper(II) bis(thiosemicarbazonato) complex formed. Cu$ATSR_3$/A-Glc complexes, **23**−**25**, have been characterized by UV/vis spectroscopy and HPLC. The EPR spectrum of complex **24** in water has also been recorded, and the copper-64-radiolabeled complex was prepared and characterized by radio-HPLC. Unfortunately, both electrospray ionization and field ionization techniques were unsuccessful, and it was not possible to obtain mass spectrometry data for any glucose-functionalized copper(II) complexes.

Diacetyl-2-(4-*N*-methyl-3-thiosemicarbazonato)-3-(4-*N*-amino-(1-β-*N*-glucosyl)-3-thiosemicarbazonato)copper(II), CuATSM/A-Glc (23). λ_{max}(H_2O)/nm 452 (ϵ/mol^{-1} dm^{-3} cm^{-1} 5229) and 305 (17 356). HPLC: R_t 5.63 min.

Diacetyl-2-(4-*N*-ethyl-3-thiosemicarbazonato)-3-(4-*N*-amino-(1-β-*N*-glucosyl)-3-thiosemicarbazonato)copper(II), CuATSE/A-Glc (24). λ_{max}(H_2O)/nm 457 (ϵ/mol^{-1} dm^{-3} cm^{-1} 5929), 360sh (7929) and 309 (15 976). HPLC: R_t 5.86 min. Radio-HPLC (^{64}Cu-**24**): R_t 9.10 and 9.30 min.

Diacetyl-2-(4-*N*-allyl-3-thiosemicarbazonato)-3-(4-*N*-amino-(1-β-*N*-glucosyl)-3-thiosemicarbazonato)copper(II), CuATSAllyl/A-Glc (25). λ_{max}(H_2O)/nm 454 (ϵ/mol^{-1} dm^{-3} cm^{-1} 5777) and 306 (19 350). HPLC: R_t 6.70 min.

DFT Calculations. All calculations were conducted using DFT as implemented in the *Gaussian03*, revision C.02, suite of ab initio quantum chemistry programs.[64] Geometry optimizations and vibrational frequency calculations were performed using the unrestricted uB3LYP exchange and correlation functionals and the double-ζ 6-31+G(d) basis set for all atoms. Normal self-consistent-field (SCF) and geometry convergence criteria were used, and no symmetry constraints were imposed. For all gas-phase calculations, harmonic frequency analysis based on analytical second derivatives was used to characterize the optimized geometries as local minima.

The effects of solvation were incorporated iteratively by performing self-consistent reaction field calculations using the integral equation formalism polarizable continuum model (IEFPCM). Geometry optimizations were performed in the presence of the reaction field using the optimized gas-phase coordinates as initial geometries. The solute−solvent boundary has been defined using a solvent-excluding surface and the United Atom Topological model (UAHF). Water (ϵ = 78.39; R_{solv} = 1.385 Å), where ϵ is the dielectric constant and R_{solv} is the sphere radius, was modeled as the solvent. A more detailed description of the calculations has been given previously.[43]

Transition energies and oscillator strengths for electronic excitation to the first 24 singlet excited states of CuATSM were calculated using TD-DFT and the unrestricted uB3LYP/6-31++G(d,p) methodology. The ground-state geometry used was reoptimized using the 6-31++G(d,p) basis set. No symmetry constraints were used in the TD−DFT calculation.

X-ray Crystallography. Crystals of **5**, **11**, and **17** were mounted on a glass fiber and cooled rapidly to 150 K in a stream of cold nitrogen using an Oxford Cryosystems CRYOSTREAM unit. Diffraction data were measured using an Enraf-Nonius Kappa CCD diffractometer (graphite-monochromated Mo Kα radiation, λ = 0.710 73 Å). Intensity data were processed using the DENZO-SMN package.[69]

Space groups were identified by examination of the systematic absences in the intensity data. The structures were solved using the direct methods program *SIR92*,[70] which located all non-hydrogen atoms. Subsequent full-matrix least-squares refinement was carried out using the *CRYSTALS* program suite.[71] Coordinates and anisotropic thermal parameters of all non-hydrogen atoms were refined. The NH hydrogen atoms were located in the difference Fourier map, and their coordinates and isotropic thermal parameters were subsequently refined. Other hydrogen atoms were positioned geometrically after each cycle of refinement. A three-term Chebychev polynomial weighting scheme was applied. Images were generated using *ORTEP-3*.[47]

For complex **12**, diffraction data were obtained using the synchrotron radiation source (λ = 0.845 70 Å) at Daresbury, U.K. The structure was solved using the same procedure as that described above.

Copper-64 Radiolabeling. Copper-64 was prepared using a biomedical cyclotron with a nickel-64 target in a procedure similar to that describe by McCarthy et al.[72] The copper-64 was extracted from the nickel-64 target as $^{64}CuCl_2$(aq) and purified from the nickel-64 using an ion-exchange column. An aqueous solution of copper-64 acetate, $^{64}Cu(CH_3CO_2)_2$, was prepared by diluting 0.2 mL of $^{64}CuCl_2$(aq) in 0.1 mol dm^{-3} HCl with 0.1 mol dm^{-3} sodium acetate (1.8 mL, pH 5.5). This stock solution was used for the radiolabeling experiments, and the activity was measured for two samples as 89.4 MBq in 2 mL and 27.0 MBq in 1 mL.

Standard solutions of the free ligand (**11**) or ZnATSE/A-Glc complex (**21**) were prepared by dissolving 0.5 mg in 1.0 mL of DMSO and deionized water, respectively.

(69) Otwinowski, Z.; Minor, W. *Methods Enzymol.* **1997**, *276*, 307.
(70) Altomare, A.; Cascarano, G.; Giacovazzo, G.; Guagliardi, A.; Burla, M. C.; Polidori, G.; Camalli, M. *J. Appl. Crystallogr.* **1994**, *27*, 435.
(71) Betteridge, P. W.; Carruthers, J. R.; Cooper, R. I.; Prout, K.; Watkin, D. J. *J. Appl. Crystallogr.* **2003**, *36* (6), 1487.
(72) McCarthy, D. W.; Shefer, R. E.; Klinkowstein, R. E.; Bass, L. A.; Margeneau, W. H.; Cutler, C. S.; Anderson, C. J.; Welch, M. J. *Nucl. Med. Biol.* **1997**, *24* (1), 35.

The copper-64 complexes **19** and **24** were prepared by reacting $^{64}Cu(CH_3CO_2)_2$ (200 μL, <10 MBq) with 50 μL or 100 μL of either the standard solution of **11** or **21** and water (400 μL) in a 2-mL reaction vial.

The reactions were stirred at room temperature for between 15 and 30 min, and then 25 μL of the reaction solution was taken for analysis by reverse-phase radio-HPLC. The syringe was washed thoroughly with DMSO and water both before and after use to prevent contamination. HPLC analysis was performed using an Agilent 1100 series HPLC machine with a 250 mm × 4.6 mm Phenomenox Primesphere 5 C18-HC 110H column. Both UV detection (λ_{obs} = 254 nm) and NaI scintillation crystal detection were used in series with a delay time of approximately 10 s. A 25-min gradient elution method was employed using a water/acetonitrile mobile-phase solvent system.

Confocal Fluorescence Microscopy. Confocal fluorescence microscopy images were recorded using a Leica DM IRBE microscope fitted with a PL APO UV 63 × 1.2 water CORR lens. Kr ion (λ_{ex} = 488 nm), Ar ion (λ_{ex} = 568 nm), Leica TCS NT lasers, and a Coherent UV laser (λ_{ex} = 365 nm) were used to excite the zinc(II) complexes studied and LysoTracker (Molecular Probes). The emission was long-pass-filtered (515 nm), and a photomultiplier tube was used for detection. Laser intensities were reduced to minimize photobleaching and any potential phototoxic effects. The microscope apparatus used has been described in more detail elsewhere.[73]

Solutions of complex **12** (1.0 mL, 0.1 mmol dm^{-3}, dissolved in 0.5% DMSO/DMEM) or complex **21** (100 μL, 1.0 mmol dm^{-3}, dissolved in water buffered at pH 7.2−7.4) were added dropwise to the extracellular medium. Fluorescence images were recorded from the time of addition.

Acknowledgment. Thanks are due to all members of the J. R. Dilworth and J. M. Peach groups at the University of Oxford. J.P.H. thanks Merton College and the EPSRC for a studentship and Dr. Min Yang for assistance with the glucose chemistry. We are indebted to Dr. Nick Rees, Colin Sparrow, and Maria Marshall for technical support and Janet Banham for assistance with EPR analysis. We thank Dr. Sofia I. Pascu for solving the crystal structure of ZnATSM/A. We thank Oksana Golovko, Dr. Katrin Probst, and Dr. Prina Ruparelia for work on the radiolabeling experiments at WBIC. We thank Dr. David K. Smith at the Department of Chemistry, University of York, for assisting with the stopped-flow kinetic experiments, and we also thank the Oxford Supercomputing Centre.

Supporting Information Available: X-ray crystallographic data for compounds **5**, **11**, **12**, and **17** (CIF format), all DFT-optimized Cartesian coordinates and molecular orbital isosurfaces of Cu(II)ATSM, and selected NMR, UV/vis, and fluorescence emission spectra and details of the gradient HPLC method. This material is available free of charge via the Internet at http://pubs.acs.org.

IC0615628

(73) Churchill, G. C.; Okada, Y.; Thomas, J. M.; Genazzani, A. A.; Patel, S.; Galione, A. *Cell* **2002**, *111* (5), 703.